

# TABLE OF CONTENT

<b>CERTIFICATION OF APPROVAL</b>		<b>i</b>
<b>CERTIFICATION OF ORIGINALITY</b>		<b>ii</b>
<b>ABSTRACT.</b>		<b>iii</b>
<b>ACKNOWLEDGEMENT.</b>		<b>iv</b>
<b>CHAPTER 1:</b>	<b>INTRODUCTION.</b>	<b>1</b>
	1.1 Background of Study.	1
	1.2 Problem Statement.	1
	1.3 Objectives and Scope of Study.	1
<b>CHAPTER 2:</b>	<b>LITERATURE REVIEW AND THEORY.</b>	<b>3</b>
	2.1 Design Phase.	3
	2.2 Fabrication Phase.	4
	2.2.1 Introduction to Welding.	4
<b>CHAPTER 3:</b>	<b>METHODOLOGY/PROJECT WORK.</b>	<b>7</b>
	3.1 CATIA V5 R6 Engineering Software.	8
	3.2 Fabrication Process.	9
	3.2.1 Gas Metal Arc Welding (GMAW).	9
	3.2.2 Cutting.	12
<b>CHAPTER 4:</b>	<b>RESULTS AND DISCUSSIONS/FINDINGS.</b>	<b>13</b>
	4.1 Go-Kart Chassis Rules and Regulation.	13
	4.2 Material Selection for Go-Kart Chassis.	14
	4.2.1 Weight.	15
	4.2.2 Strength.	15
	4.2.3 Cost.	16
	4.2.4 Ease of Manufacturing.	17
	4.2.5 Durability.	17
	4.2.6 Other Factor.	18
	4.3 Circular Tube or Rectangular Tube Selection.	18
	4.3.1 Strength of Circular versus Rectangular Tubular Structure.	19
	4.3.2 Manufacturability Comparison of Rectangular Tube and Rectangular Tube.	20
	4.4 Boundary Condition for Static Analysis.	20
	4.5 CATIA Analysis.	23
	4.5.1 Static Load Case.	24
	4.5.2 Acceleration Load Case ( $5 \text{ ms}^{-2}$ ).	27
	4.5.3 Braking Load Case ( $10 \text{ ms}^{-2}$ ).	29

4.5.4	Cornering Load Case (Clock-Wise, $a_c = 30 \text{ ms}^{-2}$ ).	31
4.5.5	Cornering Load Case (Counter-Clock Wise, $a_c = 30 \text{ ms}^{-2}$ ).	33
4.5.6	Potholes Load Case.	35
4.5.7	Bumps Load Case.	38
4.6	Impact of Addition of Two Front Torsional Bars.	40
4.7	Final Design of Go-Kart Chassis.	41
4.8	Fabrication Phase.	42
4.9	Go-Kart Chassis Homologation.	44
4.10	Testing on Chassis.	46
<b>CHAPTER 5:</b>	<b>CONCLUSION AND RECOMMENDATION.</b>	<b>49</b>
<b>CHAPTER 6:</b>	<b>REFERENCES.</b>	<b>50</b>

## LIST OF FIGURES

Figure 2.1 (a) :	Technical Drawing of Frame Subjected to FIA Homologation
Figure 2.1 (b) :	Go-kart Chassis Frame and Main Parts
Figure 2.1 (c) :	Samples of Current Go Kart Chassis Design in the Market (Azzuries Series)
Figure 3.1 :	Process Flow for Chassis Design and Construction
Table 3.2 :	The Specifications and Description of Welding Process
Figure 3.2.1 (a):	Schematic of the Gas Metal Arc Welding (GMAW) process showing torch, weld and electrical hook up.
Figure 3.2.1 (b):	Schematic of the predominant modes of molten metal transfer in the gas-metal arc welding (GMAW) process; (a) drop globular, (b) repelled globular, (c) short-circuiting, (d) projected spray, (e) streaming spray, and (f) rotating spray.
Figure 3.2.1 (c):	MIG Welding Equipment Used in the Fabrication Phase
Figure 3.2.2 :	T-Joint of Tube Frames
Figure 4.2.6 :	Graph shows the curve for loading against loading cycles for Mild Steel 1020 and Aluminium 2024
Figure 4.4 (a) :	Points of load on go kart chassis
Figure 4.4 (b) :	Free body diagram shows the forces acting on go kart seat

- Figure 4.5 : Chassis Layout for CATIA Analysis
- Figure 4.5.1.1 : Stress von Mises Analysis on Chassis after Static Loads Applied
- Figure 4.5.1.2 : Displacement Analysis of the Chassis after Static Loads Applied
- Figure 4.5.1.3 : Stress Principle Analysis on Chassis after Static Loads Applied
- Figure 4.5.2 (a): Stress von Mises Analysis on Chassis for Acceleration Load Case
- Figure 4.5.2 (b): Displacement Analysis on Chassis for Acceleration Load Case
- Figure 4.5.2 (c): Principle Stresses Analysis on Chassis for Acceleration Load Case
- Figure 4.5.3 (a): Stress von Mises Analysis on Chassis for Braking Load Case
- Figure 4.5.3 (b): Displacement Analysis on Chassis for Braking Load Case
- Figure 4.5.3 (c): Principle Stresses Analysis on Chassis for Braking Load Case
- Figure 4.5.4 (a): Stress von Mises Analysis on Chassis for Cornering (CW) Load Case
- Figure 4.5.4 (b): Displacement Analysis on Chassis for Cornering (CW) Load Case
- Figure 4.5.4 (c): Principle Stresses Analysis on Chassis for Cornering (CW) Load Case
- Figure 4.5.5 (a): Stress von Mises Analysis on Chassis for Cornering (CCW) Load Case
- Figure 4.5.5 (b): Displacement Analysis on Chassis for Cornering (CCW) Load Case
- Figure 4.5.5 (c): Principle Stresses Analysis on Chassis for Cornering (CCW) Load Case
- Figure 4.5.6 : Go Kart Chassis with Two Front Torsion Bars
- Figure 4.5.6 (a): Stress von Mises Analysis on Chassis for Potholes Load Case
- Figure 4.5.6 (b): Displacement Analysis on Chassis for Potholes Load Case
- Figure 4.5.6 (c): Principle Stresses Analysis on Chassis for Potholes Load Case
- Figure 4.5.7 (a): Stress von Mises Analysis on Chassis for Bumps Load Case
- Figure 4.5.7 (b): Displacement Analysis on Chassis for Bumps Load Case
- Figure 4.5.7 (c): Principle Stresses Analysis on Chassis for Bumps Load Case
- Figure 4.7 (a) : Orthographic View of the Go-Kart Chassis Final Design Complete with Mountings

- Figure 4.7 (b) : Upper View of the Go-Kart Chassis Final Design Complete with Mountings
- Figure 4.8 (a) : Go-Kart Chassis Fabricated Complete With Mountings
- Figure 4.8 (b) : Schematic Diagram for Calculating Throat Size,  $t$  for the Weldment
- Figure 4.9 : Go-Kart Chassis Homologation for Upper View and Side View
- Figure 4.10 (a): The Set Up of the Experiment
- Figure 4.10 (b): The Front View of the Chassis Before and After the Weight is Applied
- Figure 4.10 (c): The Chassis Set Up for Torsional Rigidity Test
- Figure 4.10 (d): The Chassis Set Up for Torsional Rigidity Test

## LIST OF TABLES

Table 1.3	:	Milestone for First Semester and Second Semester Final Year Project
Table 2.1	:	An example of Homologation for Go Kart Chassis Set by FIA
Table 2.2.1	:	Advantages and Disadvantages of Welding as a Joining Process.
Table 4.2.2	:	Comparison of properties between Aluminium and Steel
Table 4.2.4	:	Advantages of Steel for Manufacturing
Table 4.3.1	:	Torsional Shear Stress and Stiffness for Circular and Rectangular Tube
Table 4.4	:	Major Loads on Chassis with their Mass and Weight Value
Table 4.5.1	:	Summary of results for Static Load Case Analysis
Table 4.5.2	:	Results for Acceleration Load Case Analysis
Table 4.5.3	:	Results for Braking Load Case Analysis
Table 4.5.4	:	Results for Cornering (CW) Load Case Analysis
Table 4.5.5	:	Results for Cornering (CCW) Load Case Analysis
Table 4.5.6	:	Results for Potholes Load Case Analysis
Table 4.5.7	:	Results for Bumps Load Case Analysis
Table 4.6	:	The increase of Chassis Strength by Adding Two Front Torsion Bars
Table 4.8 (a)	:	List of Companies Surveyed and Fabrication Specifications
Table 4.8 (b)	:	Cost Detail for Go-Kart Chassis Fabrication
Table 4.9	:	Go-Kart Chassis Homologation (Dimensions)
Table 4.10	:	Experiment Data for Torsional Rigidity Test

## **LIST OF GRAPH**

- Graph 4.10 (a) : Force, N vs. Angle of Deflection,  $\theta$  for Actual Chassis Torsional Rigidity Test
- Graph 4.10 (b) : Force, F (N) versus Angle of Deflection,  $\theta$  (rad) for CATIA Simulation
- Graph 5.0 : Cost versus Quantity for Go-Kart Chassis

CERTIFICATION OF APPROVAL

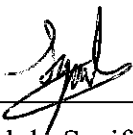
**Go-Kart Chassis Design and Construction**

By

Wan Hasni Hakimi B wan Hanafi

A project dissertation submitted to the  
Mechanical Engineering Programme  
Universiti Teknologi Petronas  
in partial fulfillment of the requirement for the  
BACHELOR OF ENGINEERING (Hons.)  
(MECHANICAL ENGINEERING)

Approved by,



---

(Mohd. Syaifudin Muhammad)

UNIVERSITI TEKNOLOGI PETRONAS

TRONOH, PERAK

July 2004

## **CERTIFICATION**

### **CERTIFICATION OF ORIGINALITY**

This is to certify that I am responsible for the work submitted in this project, that the original work is my own except as specified in the references and acknowledgements, and that the original work contained herein have not been undertaken or done by unspecified sources or persons.



---

**WAN HASNI HAKIMI B WAN HANAFI**

## ABSTRACT

This preliminary report includes an overview of the Final Year Project. The title is “Go-Kart Chassis Design and Construction”. It contains the objectives of the project, an introduction section that brief about the background, problem statement, and lastly scope of study. This report also provides some literature review and theory, findings and also the methodology in finishing the project.

The objective of the project is to design and fabricate a go kart chassis. The chassis should be lightweight, stronger and improves the existing chassis. The chassis also need to be made available at lower cost than imported chassis.

Study on chassis involved stress analysis, Finite Element Analysis and Static Mechanics. Almost every measurement aspect of design will utilize CATIA Engineering Software. For the chassis fabrication process, workshop machines will be used extensively. The chassis was fabricated by using the cutting and welding method. This method is proved to be more cost efficient but still has the characteristic of strong chassis to sustain severe conditions on tracks.

Findings on this project hopefully would be the base for future development in go-kart chassis enhancement.

## ACKNOWLEDGEMENT

I am grateful to the UTP (University Technology of Petronas) for giving me a chance to complete my Final Year Project (FYP) July 2003, which is “Go Kart Chassis Design and Fabrication” supervised by Mr. Syaifudin Muhammad.

I would like to take this opportunity to express my appreciation and thankful to those who had assisted me in making my Final Year Project (FYP) successful.

Thanks to God for His mercy for giving me time and energy to complete the project. Lots of special thanks dedicated my parents, Wan Hanafi B Wan Daud and Wan Habsah Bt. Wan Ismail, for their great support and encouragement. Much of the credit must be given to my supervisor, Mr. Syaifudin Muhammad for his tireless help and guidance throughout the whole project. His support and determination toward this project completion is worthless and deep-heartedly appreciated. Millions of thanks also dedicated to staffs at Gang Enterprise, especially Mr. Muhammad Fadzil Ishak and Mr. Johari Moin for their excellent commitment and effort in fabricating the chassis. Without them, it is almost impossible for me to complete the project. Thanks also to staffs at UTP LG Lab for their assistance and advices in the design phase of the chassis. Credits also go to these companies; City Karting, Shah Alam, Ipoh Karting Enterprise for their information and support for the project. My special thanks also goes to my beloved friends for their continuous support and encouragement to complete the project successfully; Salisa Abdul Rahman, Lukman Razali, and all individuals that have directly or indirectly assisting me in completing this project.

Last but not least, I would like to acknowledge Universiti Teknologi Petronas especially for Mechanical Department for giving me the opportunity to carry out and accomplish the project successfully.

Thanks to all.

# CHAPTER 1

## INTRODUCTION

### 1.1 Background of Study

Go-kart industry is getting popular in Malaysia as our country is keen on developing a strong motor racing industry. At an early stage of motor racing, go-kart are crucial to provide real life racing experience and a stepping stone before entering higher level of motor racing. The demand for parts and chassis of go kart is increasing each year. Suppliers for go kart parts and chassis are mostly come from Italy, which are found relatively expensive for local enthusiast. Therefore, an option for locally made spare parts and chassis is really needed for rapid growth of go kart industry in Malaysia. Some parts have been made locally but chassis are found totally imported. Development in go kart industry locally could establish a strong back bone for future enhancement of motor racing in Malaysia.

### 1.2 Problem Statement

Go-kart has been developed since decades ago in European countries and in Malaysia it is something new and growing fast. Suppliers for go-kart parts and chassis in Malaysia are monopolize by European countries, especially Italy. The chassis supplied are expensive which is price around RM16000 for each chassis. This project are meant to enable go-kart enthusiast another option for go-kart chassis which is lower in price, but light, strong and comply with the FIA regulations. Improvement on current chassis design also defines and applied to overcome several common go-kart chassis problems.

### 1.3 Objectives and Scope of Study

The main objective of the project is to design and construct a trainee go-kart chassis. This project is to understand the fundamental of a go-kart chassis, analysis and design and fabricate a chassis, which is subjected to be light, strong and durable against the normal chassis failure. For the first semester, the analysis and design of the chassis should be completed. By the second semester, the fabrication started and at the end of the project, the chassis should be ready for a complete set up of a go-kart and undergone testing.

The study on chassis involves the forces exerted on chassis internally and externally, the chassis behavior upon hard cornering, braking and accelerating and also the weight distribution on the chassis. These require a stress analysis method also static forces measurement for maximum chassis strength complying with lighter chassis. Furthermore, several designs of chassis will be developed and evaluated in finding the best feature. The best design selected will go through fabrication process, which is planned for the second semester. So, in the first semester, all work on this project will be evolved in chassis analysis and design process. This project entirely involved all mechanical static and dynamic measurement, which apply all the classroom studies and put them into practice.

In the second semester, all works are devoted in fabricating the chassis. The final design from the previous semester will be used in this process. As stated before, the best method will be used in term of manufacturability, cost efficient and also reparability.

The time frame of the project for both design phase and fabrication phase are shown in the Appendix 1-3.

## CHAPTER 2

### LITERATURE REVIEW AND THEORY

#### 2.1 Design phase

Below are an example of a go-kart chassis homologation as per FIA rules and regulation (refer Appendix 2-1(a)). At the end of the project, all these measure will be taken from the complete fabricated go-kart chassis. A sample of go-kart chassis with parts is shown in Appendix 2-1 (b).

**Table 2.1:** An example of Homologation for Go-Kart Chassis Set by FIA

Frame	Dimension	Tolerance
A = Wheel base fixed measurement	1040mm	$\pm 5\text{mm}$
B = Main tube of the structure main diameter 21mm, length over 1500mm, except lower tubes with a diameter 21mm and all the support for the accessories	1) 32mm 2) 30mm 3) 30mm 4) 30mm 5) 30mm 6) 30mm 7) 30mm	$\pm 5\text{mm}$ $\pm 5\text{mm}$ $\pm 5\text{mm}$ $\pm 5\text{mm}$ $\pm 5\text{mm}$ $\pm 5\text{mm}$ $\pm 5\text{mm}$
C = Number of bend on the tube with diameter 21mm	11	
D = Number of tube with diameter over 21mm	7	
E = Outer front width	725mm	$\pm 10\text{mm}$
F = Outer rear width	650mm	$\pm 10\text{mm}$
G = Maximum outer overall length	1505mm	$\pm 10\text{mm}$

## **2.2 Fabrication Phase**

### **2.2.1 Introduction to Welding**

The method used to fabricate the chassis is by using the cutting and welding method. Welding is a process in which materials of the same fundamental type or class are brought together and caused to join (and become one) through the formation of primary (and, occasionally, secondary) chemical bonds under the combined action of heat and pressure (Messler 1993). There are five essential points in welding which will be described below.

First and foremost is the central point that multiple entities are made one by establishing continuity. Continuity implies the absence of any physical disruption on an atomic scale, that is, no gaps, unlike with the situation with mechanical attachment or mechanical fastening where a physical gap, no matter how tight the joint, always remains. Continuity in welding does not imply the homogeneity of chemical composition through or across the joint, but it does imply the continuation of like atomic structure. When the material across the joint is not identical in composition, it is essentially the same in atomic structure, thereby allowing the formation of chemical bonds: primary metallic bonds between similar and dissimilar metals.

The second common and essential point among definitions is that welding applies not just to metals. It can and often does apply equally well to certain polymers (e.g. thermoplastics), crystalline oxide or nonoxide ceramics, intermetallic compounds, and glasses. The process being performed may not always be called welding. It may be called thermal bonding for thermoplastics, or fusion bonding or fusion for glasses, but it is still welding.

The third essential point is that welding is the result of combined action of heat and pressure. Welds can be produced over a wide spectrum of combinations of heat and pressure: from essentially no pressure when heat is sufficient to cause melting, to where pressure is great enough to cause gross plastic deformation when no heat is added and

welds are made cold. Welding is a highly versatile and flexible joining process, enabling the joining of many different materials into many different structures to obtain many different properties for many different purposes.

The fourth essential point is that an intermediate or filler material of the same type, even if not same material, as the base material may or may not be required. The option of employing an intermediate or filler or not adds to process flexibility and versatility.

The fifth and final essential point is that welding is used to join parts, although it does so by joining material. Creating a weld between two materials requires producing chemical bonds by using some combination of heat and pressure. This is the characteristic which is often determined the selection of welding process. Heat and pressure required for welding depends partially by inherent nature of the material being joined. It also depends on the nature of the actual parts or physical entities being joined. Other factors are part shape, critical part dimensions, and part properties that must be dealt with by preventing intolerable levels of distortion, residual stresses, or disruption of chemical composition and microstructure. The main point is that welding is a secondary manufacturing process used to produce an assembly or structure from parts or structural elements.

Below summarizes the advantages and the disadvantages of welding as a joining process.

**Table 2.2.1:** Advantages and Disadvantages of Welding as a Joining Process. (From R. W. Messler's *Joining of Advanced Materials*, Table 6.1, published in 1993 by Butterworth-Heinemann, Stoneham, MA)

Advantages	Disadvantages
1. Joints of exceptional structural integrity and efficiency, will not accidentally loosen or disassemble	1. Impossible to disassemble joints without destroying detail parts
2. Wide variety of process embodiment	2. Heat of welding degrades base properties
3. Applicable to many materials within a class	3. Unbalanced heat input leads to distortion or residual stress
4. Manual or automated operation	4. Requires considerable operator skill
5. Can be portable for indoor or outdoor use	5. Can be expensive (e.g. thick sections)
6. Leak-tight joints with continuous welds	6. Capital equipment can be expensive
7. Cost is usually reasonable	

## CHAPTER 3

### METHODOLOGY/PROJECT WORK

#### 3.1 Methodology/Project flow

Methodology in completing the project is presented in flow chart below:

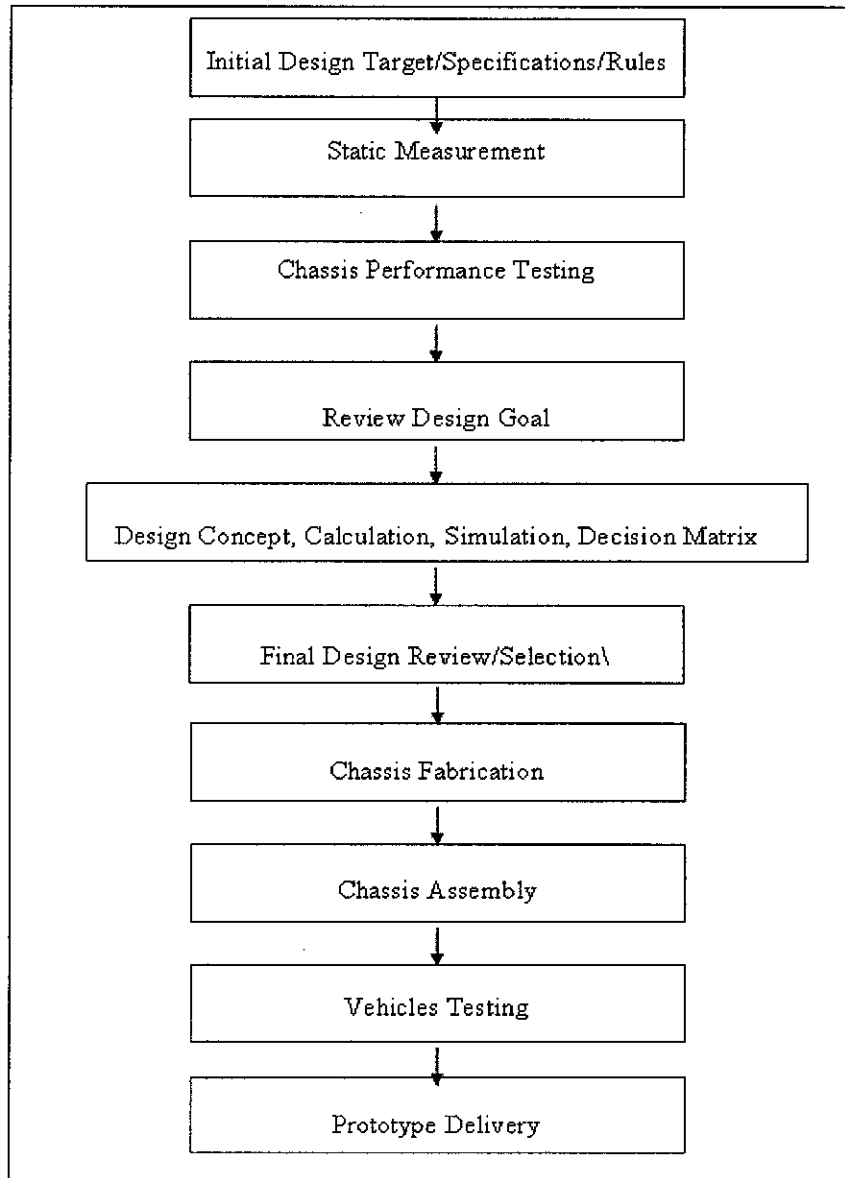


**Figure 3.1:** Process Flow for Chassis Design and Construction

Tools need to be use:

- i. CATIA Engineering Software
- ii. Workshop Machines

### **3.1 CATIA V5 R6 Engineering Software**

By using this software, one able to create and design structure and also simulate it according to the real world. In designing the final chassis design, a lot of time spent using this software. The process kicks off with determining the limit of certain essential dimension of the chassis in 2D environment. After the line frame of chassis drawing completed, the line was then lofted according to the outer diameter of the solid tube. After the solid tube generated, it was then shelled according to the thickness desired for the tube frame. When the bare frame completed, several load points was created on certain area, which was determined in earlier staged. This load points generally represents the loads of driver, petrol and engines attached to the chassis. After it was completed, the design was then transferred to generative and meshing simulation.

In this simulation part, the loads were applied to the chassis base on earlier calculation on the load points. After that, calculation by using the software begin and the result can be manipulated to get the stresses built up in the chassis, the displacement after loads applied and also the principle stresses in the chassis. The simulation also showed the most severe area of the chassis which experienced the highest stress and also greatest displacement. From several simulations, the chassis underwent several modifications to eliminate the weaknesses. Such efforts were adding two front torsion bars at the upper part of the chassis, which is identified to have the highest stress built up.

After the results of several simulations were obtained, and the resultant stresses are within the desired target, then the final design for the chassis was completed. The results of the simulation are represented in the result section of this report.

## 3.2 Fabrication Process

### 3.2.1 Gas-Metal Arc Welding

The gas-metal arc welding (GMAW) or so called metal-inert gas (MIG) process employs a continuous consumable solid wire electrode and an externally supplied inert gas shielding. A schematic of the process is shown in Figure 3.2.1 (a). The consumable wire electrode produces an arc with the work piece made part of the electric circuit and provides filler to the weld joint. The wire is fed to the arc by an automatic wire feeder, of which both push and pull types are employed, depending on the wire composition, diameter, and welding application.

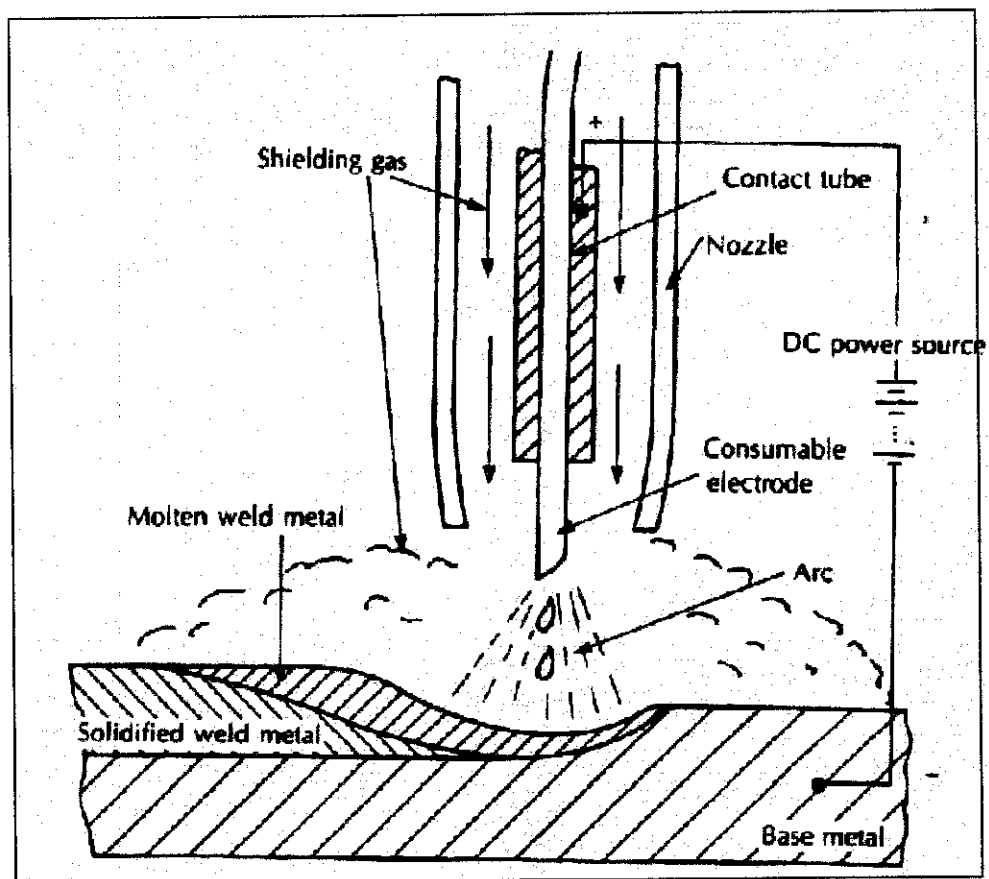


**Figure 3.2.1 (a):** Schematic of the Gas Metal Arc Welding (GMAW) process showing torch, weld and electrical hook up. (From *Joining of Advanced Materials* by R. W. Messler, Jr., published in 1993)

The externally supplied shielding gas plays dual roles in GMAW. First, it protects the arc and the molten or hot, cooling weld metal from air. Second, it provides desired arc characteristic through its effect on ionization. A variety of gases can be used, depending on the reactivity of the metal being welded, the design of the joint, and the specific arc characteristic that are desired.

Constant voltage DC arc welding power supplies can be used, hooked up as shown in Figure 3.2.1 (a). Either DCSP (DCEN) or DCRP (DCEP) may be used, depending on the particular wire and desired mode of molten metal transfer, but the DCRP (DCEP) mode is far more common. The reason is that in the RP mode, electrons from the negative work piece strike the positive wire to give up their kinetic energy in the form of heat to melt and consume the wire. The heat given up to the wire to melt it is recovered to help make the weld when the molten metal from the wire is transferred to the work piece.

A distinct advantage of GMAW is that the mode of molten metal transfer from the consumable wire electrode can be intentionally changed and controlled through a combination of shielding gas composition, power source type, electrode type and form, arc current and voltage, and wire feed rate. There are three predominant metal transfer modes; spray, globular, and short-circuiting. The characteristic of the molten metal for each mode is shown in Figure 3.2.1 (b).

In summary, the GMAW process offers flexibility and versatility, requires less manipulative skill, and enables high deposition rates (5-20kg per hour) and efficiencies (80-90%); referring to which energy is transferred from the heat source to the work piece for use in making the weld. The greatest shortcoming of the process is that the power supplies typically required are expensive. (Refer Appendix 3-2 for welding specifications used in this project)

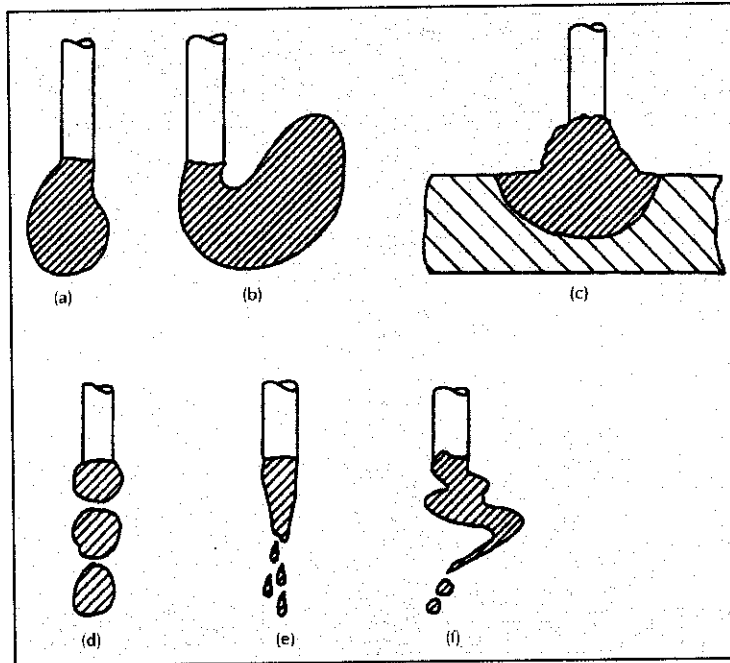


**Figure 3.2.1 (b):** Schematic of the predominant modes of molten metal transfer in the gas-metal arc welding (GMAW) process; (a) drop globular, (b) repelled globular, (c) short-circuiting, (d) projected spray, (e) streaming spray, and (f) rotating spray. (From *Joining of Advanced Materials* by R. W. Messler, Jr., published in 1993)

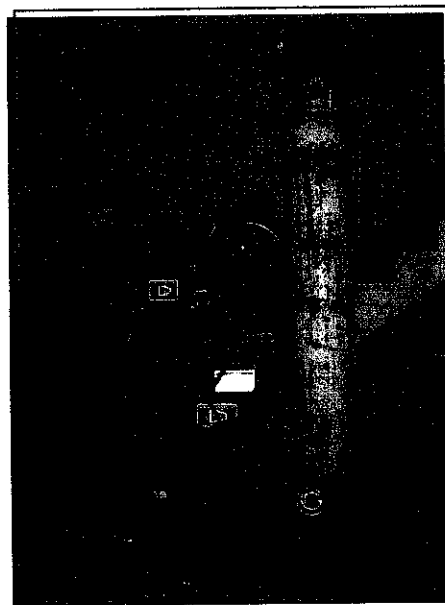


**Figure 3.2.1 (c):** MIG Welding Equipment Used in the Fabrication Phase

### 3.2.2 Cutting

Based on the design, the material will be undergone cutting before being weld together. The cutting process involved two steps. The first step is cutting the tube into the desired dimension by using a cut-off machine. The rough cutting into its desired dimension will cause rough cut surface which is then grinded to achieve smooth surface. Before welding could be done, the angles of the tube joining the subsequent tube are measured first. This is in order to achieve only 2 mm tolerance between joining before welding started. Furthermore, the tube that has been cut will have to follow the subsequent surface; e.g. semi rounded end tube. This applied to all tubes joining in cross section. The illustration for the above case is shown below. The arrow indicates the symbol for groove weld with complete penetration.

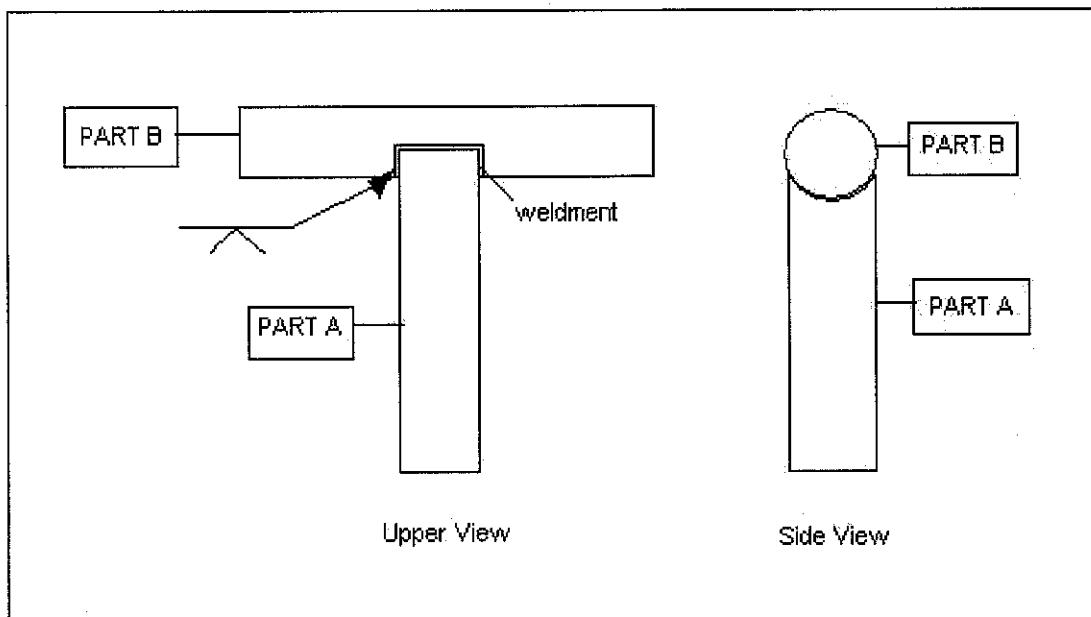


**Figure 3.2.2:** T-Joint of Tube Frames

As illustrated above, the upper end of Part A has to be cut according to curve of Part B. This is only an example for a simple T- joint between these tubes.

## CHAPTER 4

### RESULT AND DISCUSSION/FINDINGS

#### 4.1 Go Kart Chassis Rules and Regulation

Below are the specifications for go-kart chassis, which comply with FIA Rules and Regulation.

Chassis specifications:

1. Frame must be similar in design and appearance to a down tube sprint car. Total dimensions of the kart may not exceed a length of 98" and width of 54" at any point. Maximum kart height 72" measured from the highest point on the wing. Kart must provide a minimum of 3" between top of drover's helmet and the top of roll cage (bolt on or weld on cage extensions will be acceptable to maintain these clearances. Tubing used must be same diameter and material as mainframe tubing).
2. Main frame must be constructed of minimum .062 wall thickness, one inch OD 1020 electric weld mild steel tubing or material of equal or greater strength, minimum 1" OD round tubing only.
3. Must have an "A" frame behind driver's seat. The main frame must be welded, no slip joints.
4. Nerf bars, front and rear bumpers must be ¾" OD minimum with .065" minimum wall thickness mild steel. No Aluminum allowed. Front bumper to be a minimum of 12" off the ground. Rear bumper must be double rail design with lowest point a maximum of 9" off the ground. Nerf bars must be double rail design with top nerf bar a minimum of 12" off the ground. Extra bars are recommended for motor protection.
5. Optional suspension system must be coil over design with Azusa shock #1700-136 as manufactured. No modifications allowed. It must not travel over 2 ½". All suspension parts must be keyed or safety wired. Place steel washer on each side of rubber grommet on both ends of shock to prevent pull-out. NOTE: kart must fall to the ground when shocks are removed.
6. Rear axle must be one piece, no differentials.

7. Front axle must have a positive stop to control upward movement if legs are over front axle.
8. Wheel base 42" minimum to 63" maximum.
9. No mirrors allowed.
10. Karts will have no sharp edges or protrusions that may cause injury to a competitor or themselves.
11. All karts must have a mandatory kill switch.
12. No part of the kart chassis may be adjusted while the kart is in motion.
13. Seat must be high back aluminum.
14. Wheels shall be void of any defects. Maximum number of 4 wheels
15. Tires front and rear, must be 5" or 6" diameter go-kart tires.

The specifications of go kart chassis is clearly stated above. Designing a go kart chassis complying with all the rules and regulation set by FIA is important for safety and recognition by other manufacturer. Every detail will be complied to ensure the go kart design in this project is within the FIA rules and regulations.

#### **4.2 Material Selection for Go Kart Chassis**

Rules and regulation of go-kart limit the minimum yield strength of the material is the yield strength for Mild Steel 1020, which is 345 MPa. Higher yield strength materials are allowed. Steel is already well established in structure design for their special physical properties and the advance research in the material.

Nowadays, as research on material developed, aluminium alloys has find its way into the structure industries. Aluminium alloys has the advantage of lightweight, but still unable to compare with steel in term of strength. In this report, comparison between steel alloy and aluminium alloy will be discussed and the result of the selection was concluded.

Materials selected for comparison in this report are Mild Steel 1020 and Aluminium Alloy 2024. Comparisons are done in six aspects:

- 1) Weight
- 2) Strength
- 3) Cost
- 4) Ease of Manufacturing
- 5) Durability
- 6) Other factors

#### **4.2.1 Weight**

Aluminium alloy has density of  $2.77 \text{ g/cm}^3$  while steel alloy density is  $7.85 \text{ g/cm}^3$ . From this value alone, we could know that aluminium usage reduced almost 60% than its steel counterpart. In weight factor, design of chassis is preferable to aluminium.

#### **4.2.2 Strength**

Strength is defined as the ability of a material to withstand a force without breaking or permanently deforming. Strength is commonly known as yield strength in engineering term. In comparison between the two metallic alloys, the yield strength of Mild Steel 1020 is found slightly higher to Aluminium Alloy 2024. However; there are many other options for steel of higher strength. Heat treatment, annealed and tempering process could shoot up the yield strength of steel to over 1000MPa. Because the process for steel treatment is already in advance state, steel is known to have the inferior properties in term of strength over aluminium. Strength factor are important to make sure that the chassis do not fail during aggressive driving and also durable to cyclical stress failure.

A list of properties for both metallic materials is shown in Table 2.

**Table 4.2.2:** Comparison of properties between Aluminium and Steel

Properties	Aluminium Alloy 2024	Mild Steel 1020
Yield Strength (MPa)	345	380
Tensile Strength, $\sigma$ (MPa)	470	440
Fracture Toughness (MPa.m <sup>1/2</sup> )	44	76
Modulus of Elasticity, E (GPa)	72.4	207
Shear Strength, $\tau$ (MPa)	280	205
Modulus of Rigidity, G(GPa)	26	77

#### 4.2.3 Cost

Material cost is important to determine the material selection. Generally, steel is cheaper than aluminium. As an example, aluminium cost is about \$11.00/kg for Aluminium Alloy 2024 as cast, custom pieces meanwhile stainless steel is \$1.45/kg for Steel Alloy 1020 (cold rolled). Although aluminium ore are abundant the extraction cost of pure aluminium is very energy intensive, being electro chemical in nature rather than the purely chemical process used for steel. Thus pure aluminium is more expensive than steel and has lower inherent strength and stiffness. This cost factor prefers steel over aluminium for chassis material.

#### 4.2.4 Ease of Manufacturing

Comprehensive ways of modeling the performance of current steel structure are widely known. Compared to aluminium modeling, the process is still in learning phase of how to model aluminium structures.

- Steel manufacturing has already been in advance level nowadays. Aluminium is quite new technology in automotive industries.
- The initial and manufacturing cost for stainless steel is lower than the aluminium. The material is also versatile, evolving along breakthrough of technology.
- Thus the stainless steel is superior in ease of manufacturing factor.
- Other advantages of steel are put into Table 3 below:

**Table 4.2.4: Advantages of Steel for Manufacturing**

Properties	Benefit
Balance of strength and formability	Design flexibility
Easier handling	Higher quality, low cost
Better spot weldability	Higher quality, low cost
Obvious fatigue limit	Easier design
Fewer problems with galvanic corrosion	Easier design

#### 4.2.5 Durability

Durability in terms of resistance to cyclic stresses is another area where, in practice, limitations of aluminium alloys are exposed. The lack of endurance limit for aluminium alloys means that aluminium structure subjected to cyclic loading require more rigorous testing to ensure that they would not suffer a fatigue failure. A sample for stress against number of cycles represent below in Figure 1. It is clear that steel is slightly more durable than aluminium against cyclic loading.

#### 4.2.6 Other factor

The ease of handling, resistance welding and repair of chassis damage are also advantages of steels over alternatives material.

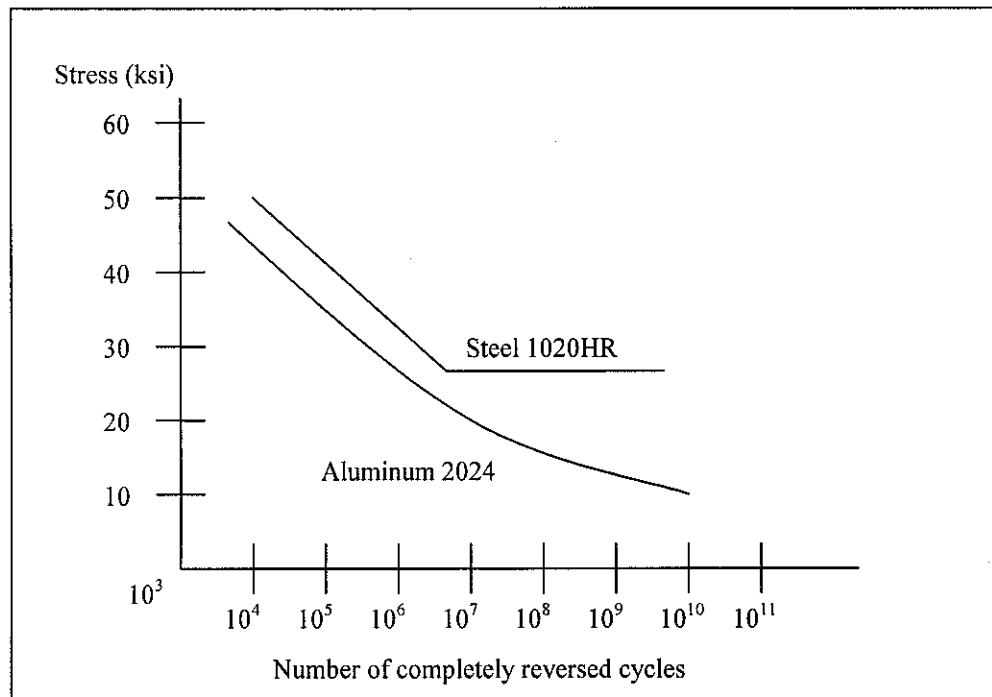


**Figure 4.2.6:** Graph shows the curve for loading against loading cycles for Mild Steel 1020 and Aluminium 2024

After all of these factors have been taken into consideration, Mild Steel 1020 was selected. Though it has larger weight than aluminium, it still performs the best option in term of cost efficiency and ease of manufacturing.

#### 4.3 Circular Tube or Rectangular Tube Selection

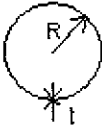
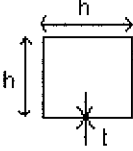
Go kart chassis are usually made of tubular circular structure. In this project, the constraint of time and fund restricted the development to consider the cheaper and more manufacturability alternative which is rectangular tubular chassis. In this report, the alternatives are considered in term of:

- Strength
- Manufacturability
- Cost efficient

### 4.3.1 Strength of Circular versus Rectangular Tubular Structure

Formulae for finding shear strength;  $\tau$  and torsional stiffness constant of these two structures are simplified in Table 4 according to the tubular shape.

**Table 4.3.1:** Torsional Shear Stress and Stiffness for Circular and Rectangular Tube

Cross Section	Shear Stress, $\tau$	Torsional Stiffness Constant, J
	$\tau = \frac{T}{2 \pi R^2 t}$	$J = 2 \pi R^3 t$
	$\tau = \frac{T}{2 h^2 t}$	$J = h^3 t$

As the formulae for finding the stress and torsional stiffness showed above, a comparison between the two types of thin wall structure can be seen. For the same value of torque, T the shear stress build up for circular tube are governed by the factor of  $2 \pi R^2 t$  while for rectangular tube is  $2 h^2 t$ . From this factor, it can be clearly being seen that shear stress experienced by rectangular are bigger than circular tube. These indicate that circular tube will yield lower shear stress build up than rectangular. For torsional stiffness, J a bigger value indicates the ability of the structure to withstand larger value of torsion. Even in this factor, circular tube are superior that rectangular tube. Therefore, using a circular tube clearly is an advantage in strength factor.

### **4.3.2 Manufacturability Comparison of Rectangular Tube and Rectangular Tube**

It was found that the rectangular tube is easier to manufacture than circular tube. This is caused by the bending parts of the chassis. The bending part of the could be constructed by simply cutting the rectangular tube into desired angle and weld them together. Comparing with the rectangular tube, bending circular tube needs heating process to bend them into shape, which will cost more and harder to construct. Sharp bends for rectangular tube will affect overall performance of strength of the chassis. The forces build up will certainly higher at the bend sharp corners than smooth bend of circular tube. By considering the factor of time constraint and the ease of manufacturability, rectangular tube structure is favorable but compromising the strength of the chassis.

### **4.4 Boundary Condition for Static Analysis**

Analysis on go-kart chassis will be dealt in several conditions:

- Static Analysis
- Cornering
- Braking
- Acceleration

In each of these case, forces involve in the chassis was calculated. The value calculated will be used as the boundary condition for later analysis using CATIA software.

For the static forces, several major loads were calculated. These values are:

- Driver weight
- Complete engine weight with exhaust system
- Rear axle weight
- Petrol tank weight

These values are important in setting up the boundary condition of the chassis by using the CATIA software. These boundary values will later on determined the stresses built up in the

chassis together with the deflection of each beams of the chassis. These values are obtained during the visit to Shah Alam Go-Kart Centre on 29 September 2003.

The weight for parameter is shown in Table 4.4 below. The value of gravity acceleration,  $g$  is  $9.81 \text{ ms}^{-2}$ . The driver weight taken is above average weight whereas considered as the worst case condition. This also applies to other parameters.

**Table 4.4: Major Loads on Chassis with their Mass and Weight Value**

Parameter	Mass, kg	Weight, N ( $m \times g$ )
Driver	80	784.8
engine	20	196.2
Rear axle	5	49.05
Petrol	5	49.05

Points where the weight forces applied to the go kart chassis are shown in Figure 4.4 (a).

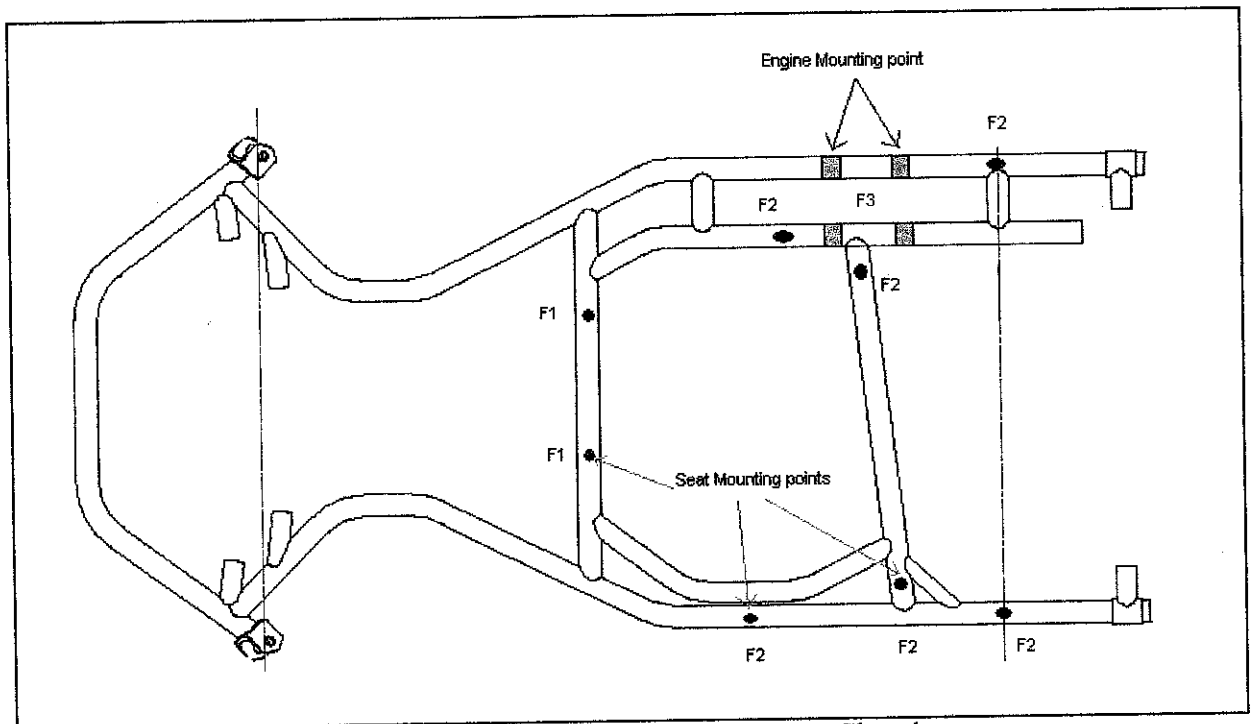


**Figure 4.4 (a): Points of Load on Go Kart Chassis**

The value for each force has been calculated by using the equilibrium method. Whereas, in static analysis case, value involved are in vertical direction. Summary of forces calculated are given below:

$$F1 = 192.6 \text{ N}$$

$$F2 = 65.4 \text{ N}$$

For value  $F1$  and  $F2$ , the seat shape is first determined. The free body diagram for seat is shown in Figure 4.4 (b) below:

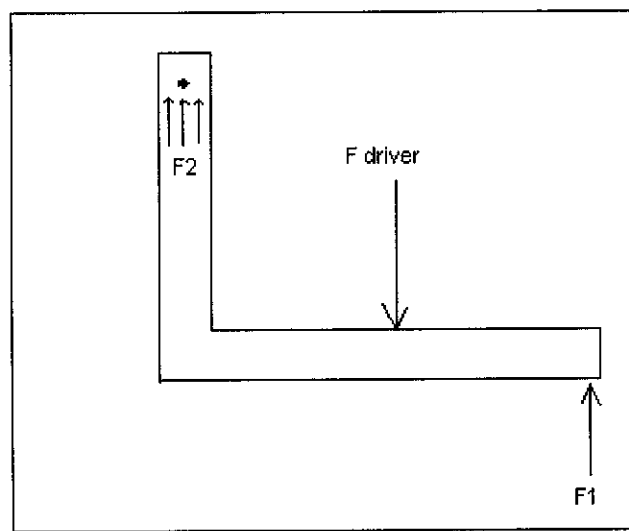


**Figure 4.4 (b):** Free Body Diagram Shows the Forces Acting on Go Kart Seat

Considering only the vertical forces on the seat, values of  $F1$  and  $F2$  were obtained. From the major parameter of mass load on chassis, the drivers' weight obviously the largest weight than others. Weight of the driver is observed to be distributed on 8 points on the chassis (See Figure 4.4 (a)). The second largest weight is the engine. The mounting position of the engine is also shown in Figure 4.4 (a). The engine is mounted by using upper and lower clamp bolted together gripping the chassis body.

#### 4.5 CATIA Analysis

After the boundary conditions were calculated, CATIA Software was used to evaluate the Stress Von Mises, displacement and also principle stresses. The chassis design used for the analysis is shown below. This is the basic chassis layout for the project. From this point, adjustment and modification will be made to eliminate any weaknesses on the chassis such as high stress built up on certain area of the chassis. From the analysis on the chassis below, summary of findings of analysis are stated in subsections.

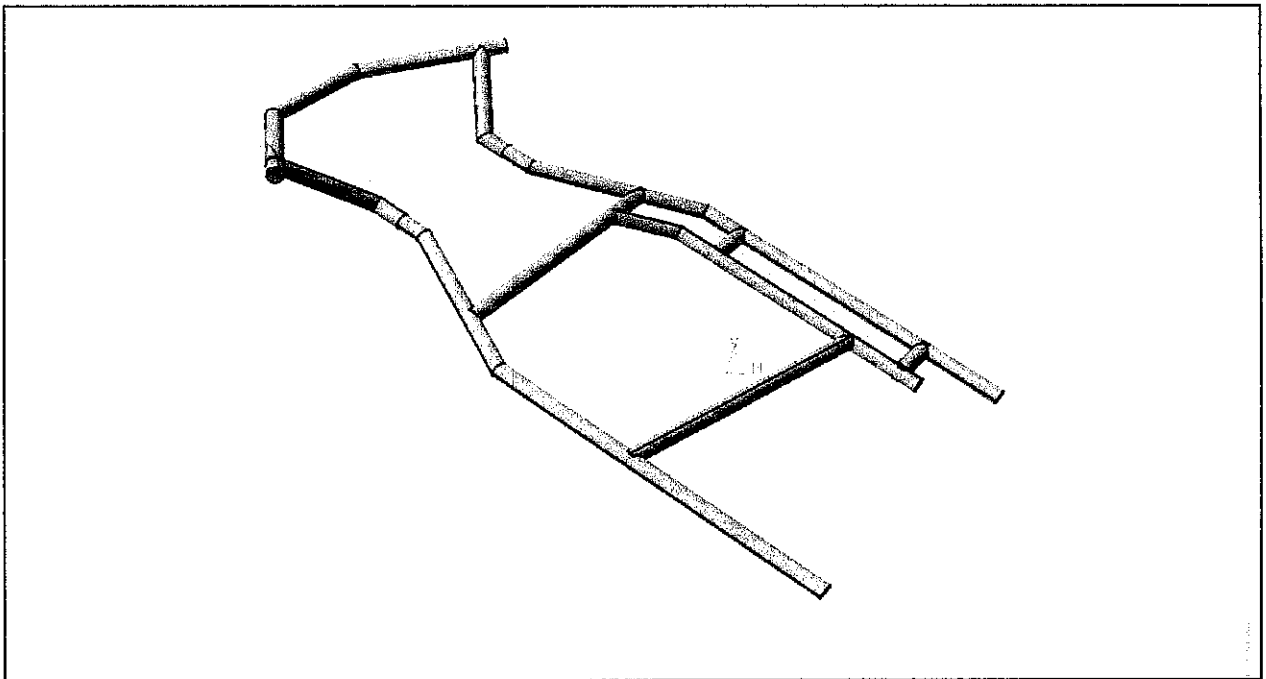


**Figure 4.5:** Chassis Layout for CATIA Analysis

Material used for the analysis is Mild Steel 1020. The front and rear tire axle are considered the fix point as it opposed any force exerted from driver, engine and other loads defined earlier in this report.

## 4.5.1 STATIC LOAD CASE

### 4.5.1.1 Stress Von Mises Analysis

As the figure shows above, a slight deformation of the chassis can clearly be seen. This is due to the static load applied to the chassis. According to the *von Mises Criterion*, a given structural components is safe as long as the maximum value of the distortion energy per volume in that materials remain smaller than the distortion energy required to cause yield. As noted earlier, the value is 77GPa.

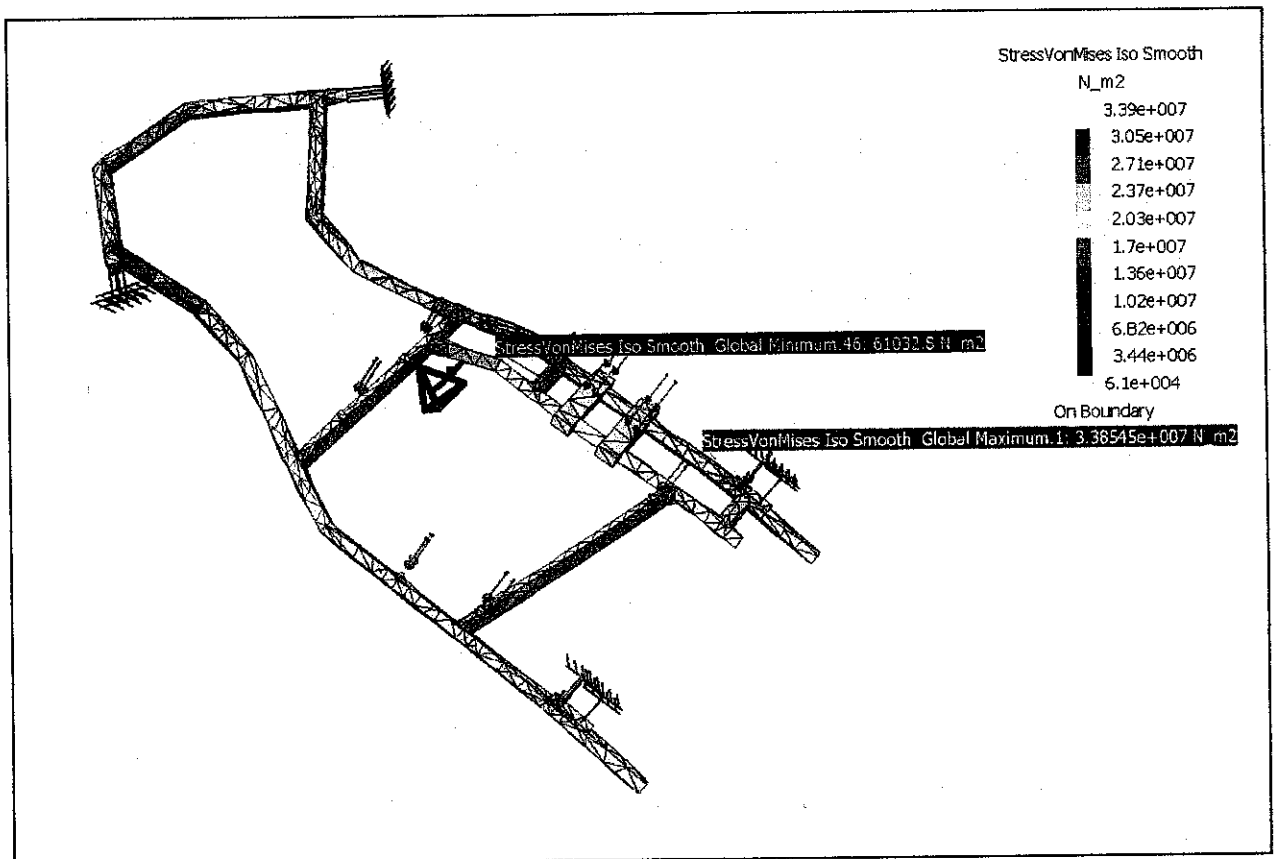


**Figure 4.5.1.1:** Stress von Mises Analysis on Chassis after Static Loads Applied

#### 4.5.1.2 Displacement Analysis

From the analysis above, it was found that the maximum displacement occurred at the beam supported most of the drivers' weight. The displacement value is 0.0924mm. As stated earlier, the fix point on the chassis are the rear and front axle. Thus, there's no displacement occurred at these two points.

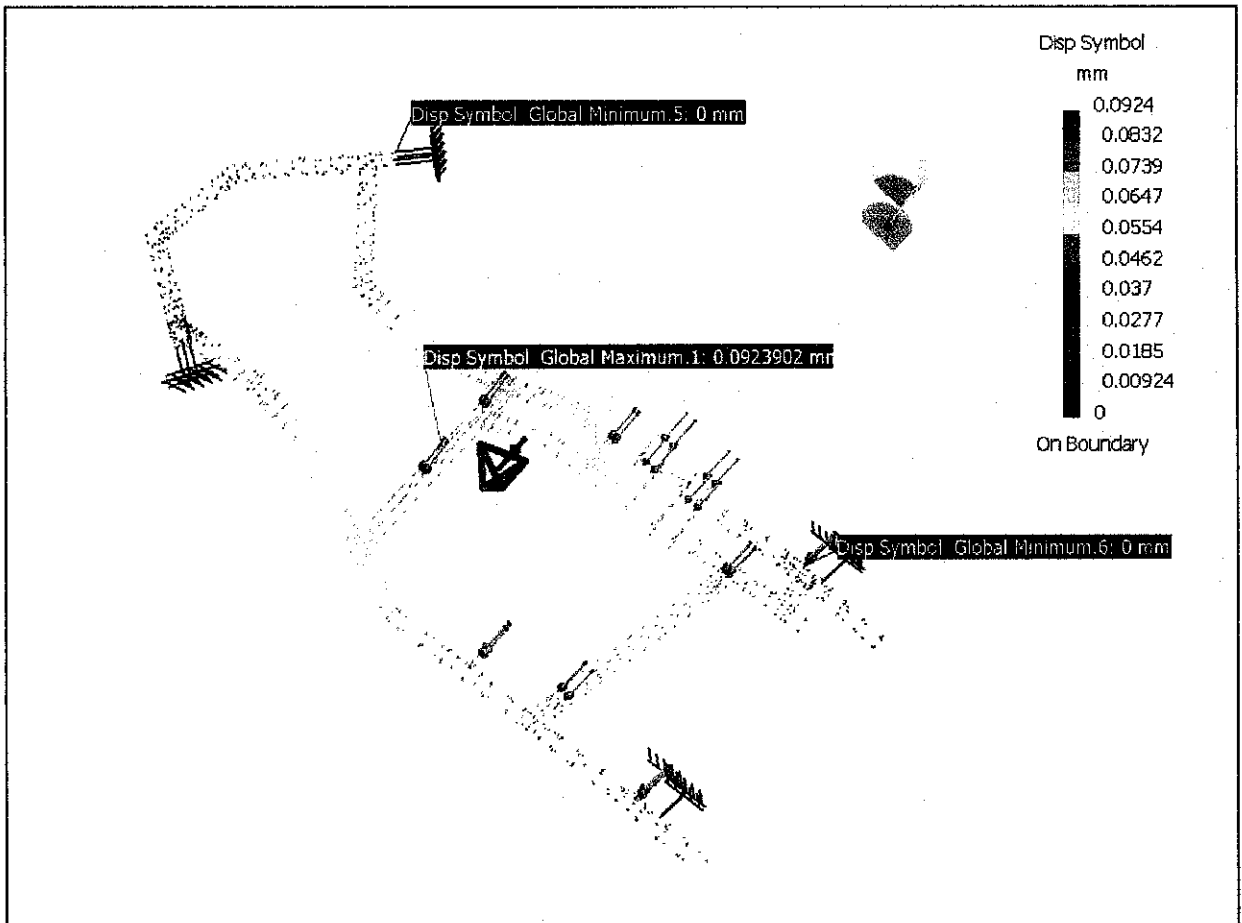


**Figure 4.5.1.2:** Displacement Analysis of the Chassis after Static Loads Applied

### 4.5.1.3 Principle Stresses Analysis

From the figure above, the minimum and maximum of principle stress are shown. The value of principle stresses is important to determine the distortion energy per unit volume of the structure. It is also important to determine the maximum shearing stress,  $\tau$  occurred in the structure.

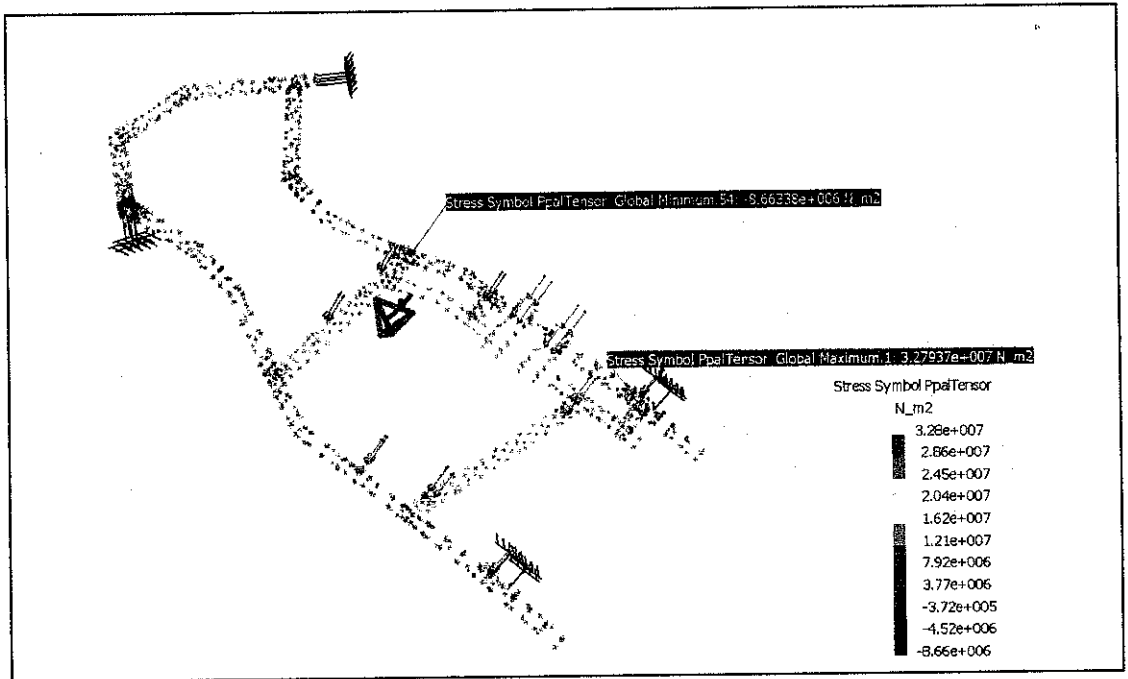


Figure 4.5.1.3: Stress Principle Analysis on Chassis after Static Loads Applied

Table 4.5.1: Summary of results for Static Load Case Analysis

State Analysis	Measure	Location
Maximum Stress, $\text{Nm}^{-2}$	$3.39 \times 10^7$	Right region of rear axle with side frame
Maximum Displacement, mm	0.0924	Middle of centre frame
Principle Stresses, $\sigma$	Max. $3.28 \times 10^7$ Min. $-8.66 \times 10^6$	- Joint of right rear axle with side frame - Joint of right side frame with centre tube frame

### 4.5.2 ACCELERATION LOAD CASE (5ms<sup>-2</sup>)

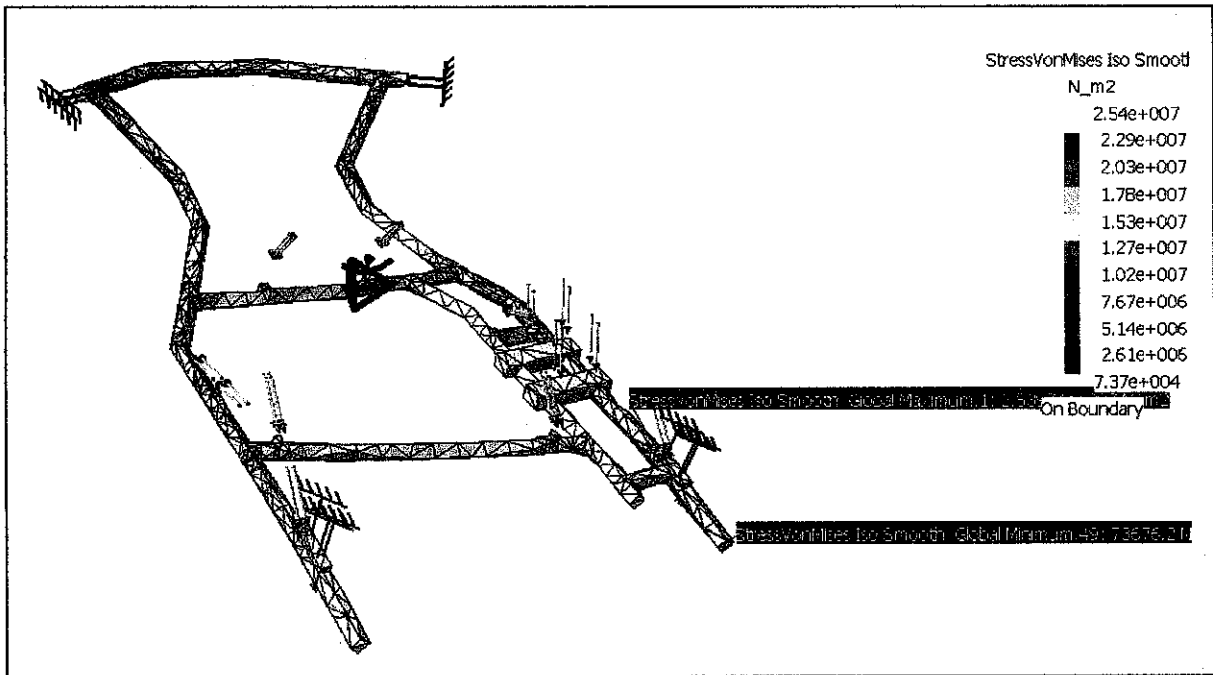


Figure 4.5.2 (a): Stress von Mises Analysis on Chassis for Acceleration Load Case

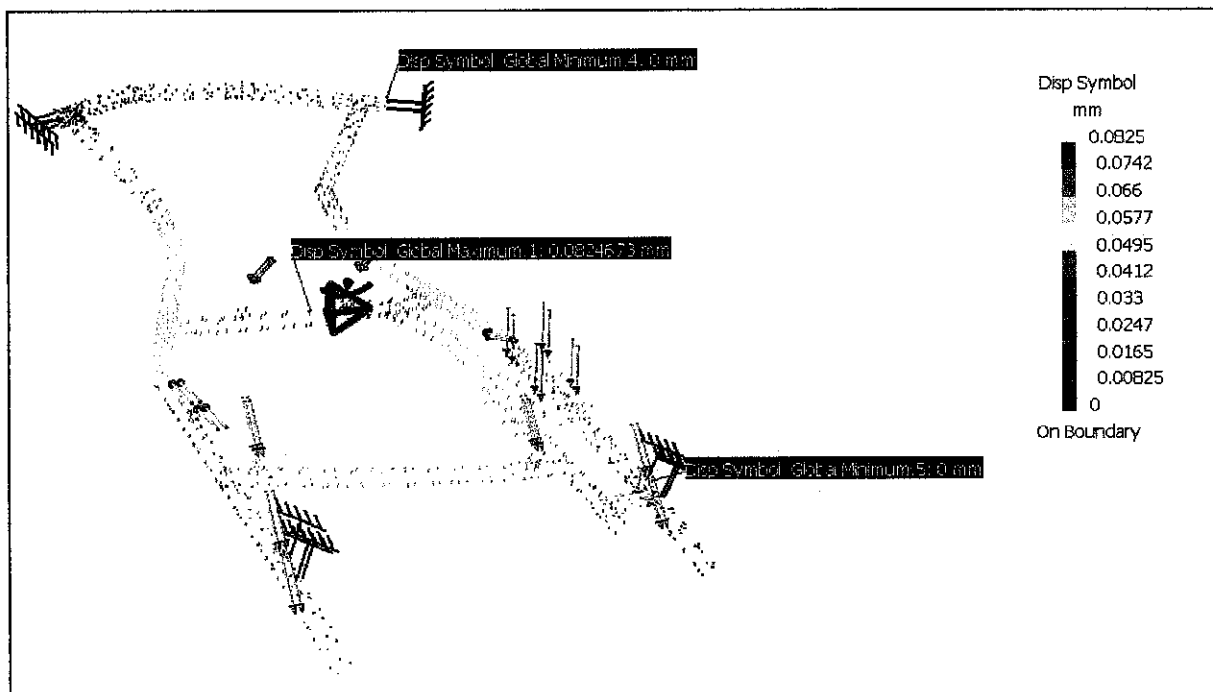


Figure 4.5.2 (b): Displacement Analysis on Chassis for Acceleration Load Case

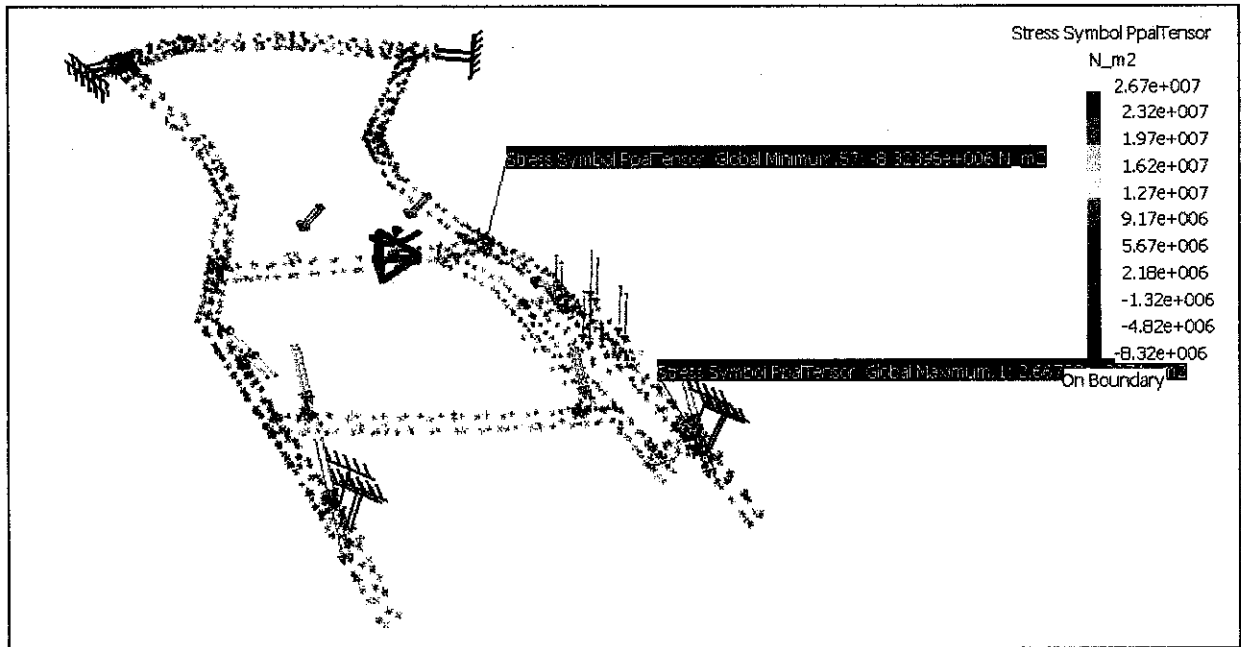


Figure 4.5.2 (c): Principle Stresses Analysis on Chassis for Acceleration Load Case

Table 4.5.2: Results for Acceleration Load Case Analysis

State Analysis	Measure	Location
Maximum Stress, $\text{Nm}^{-2}$	$2.54 \times 10^7$	Region of right rear axle joint with side frame
Maximum Displacement, mm	0.0825	Middle of centre frame
Principle Stresses, $\sigma$	Max $2.67 \times 10^7$ Min $-8.23 \times 10^6$	- Joint at right rear axle with side frame - Joint of centre tube to the right side frame

### 4.5.3 BRAKING LOAD CASE ( $10\text{ms}^{-2}$ )

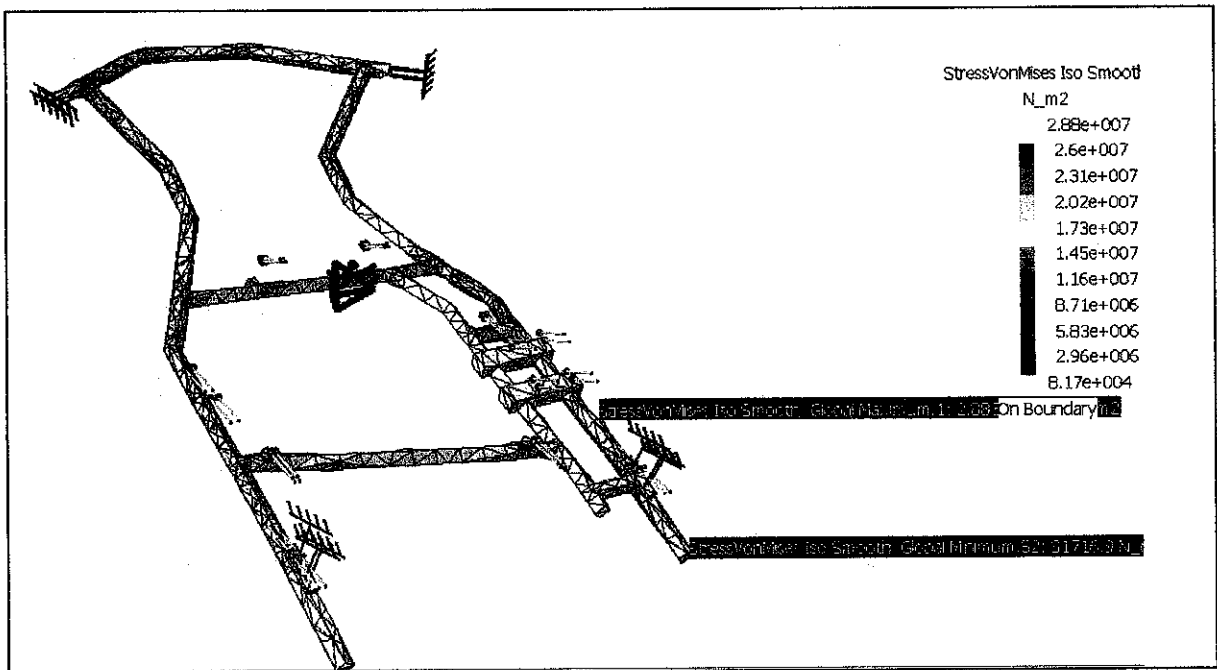


Figure 4.5.3 (a): Stress von Mises Analysis on Chassis for Braking Load Case

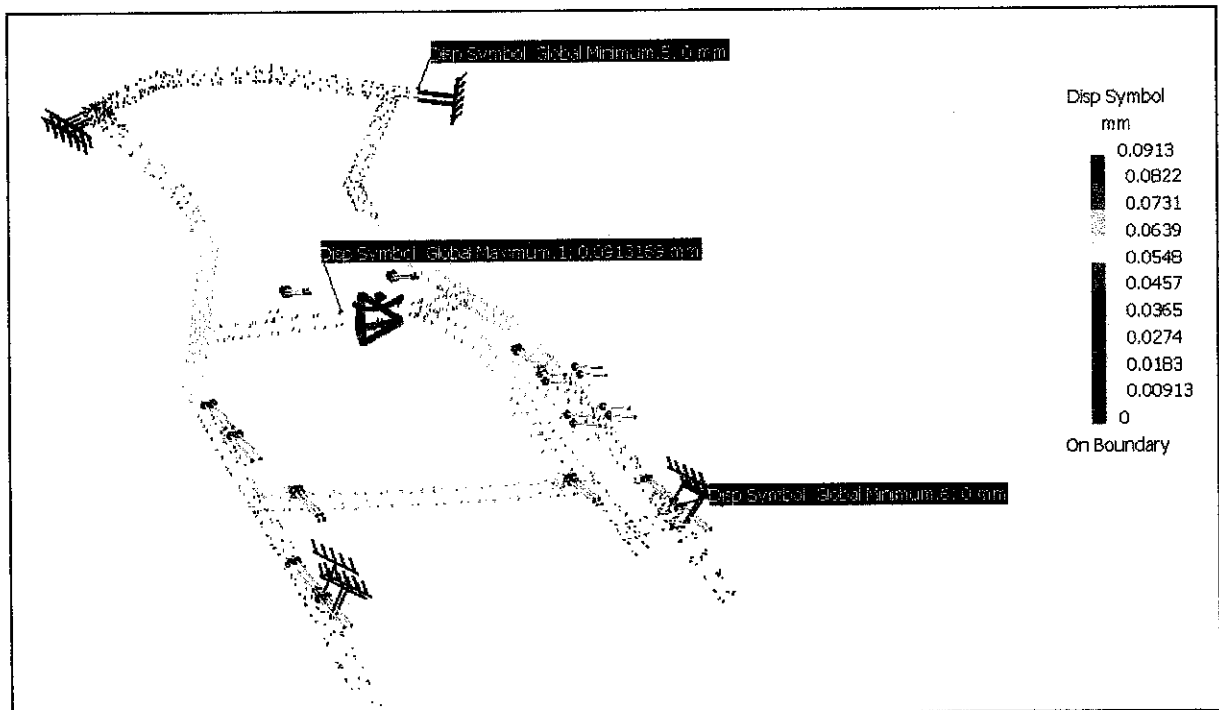


Figure 4.5.3 (b): Displacement Analysis on Chassis for Braking Load Case

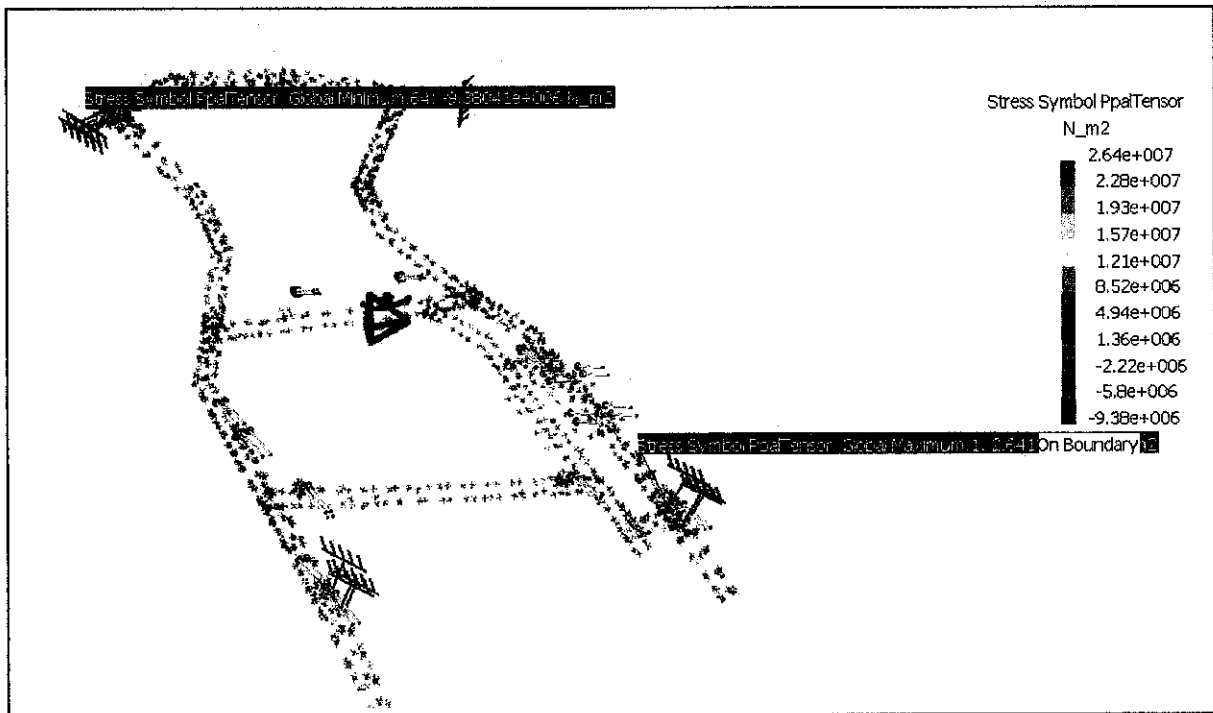


Figure 4.5.3 (c): Principle Stresses Analysis on Chassis for Braking Load Case

Table 4.5.3: Results for Braking Load Case Analysis

State Analysis	Measure	Location
Maximum Stress, $\text{Nm}^{-2}$	$2.88 \times 10^7$	Region of right rear axle joint with side frame
Maximum Displacement, mm	0.0913	Middle of centre frame
Principle Stresses, $\sigma$	Max $2.64 \times 10^7$ Min $-9.38 \times 10^6$	- Joint at right axle with side frame - Joint of centre tube to the right side frame

#### 4.5.4 CORNERING LOAD CASE (CLOCK WISE, $a_c = 30\text{ms}^{-2}$ )

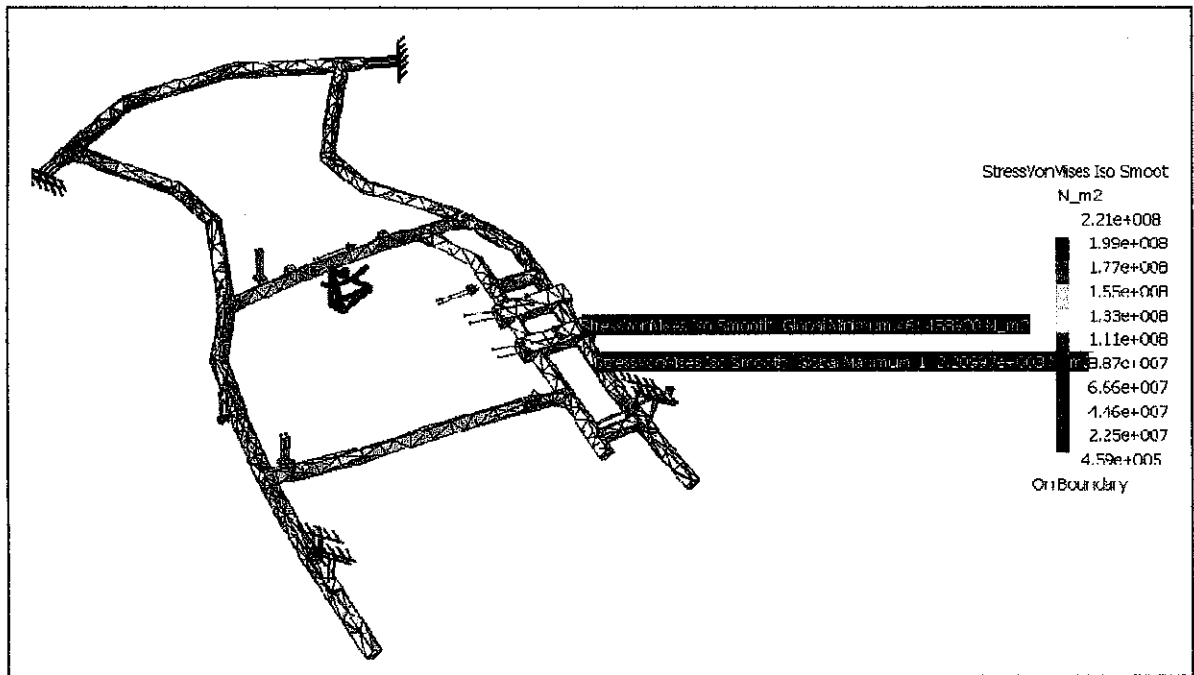


Figure 4.5.4 (a): Stress von Mises Analysis on Chassis for Cornering (CW) Load Case

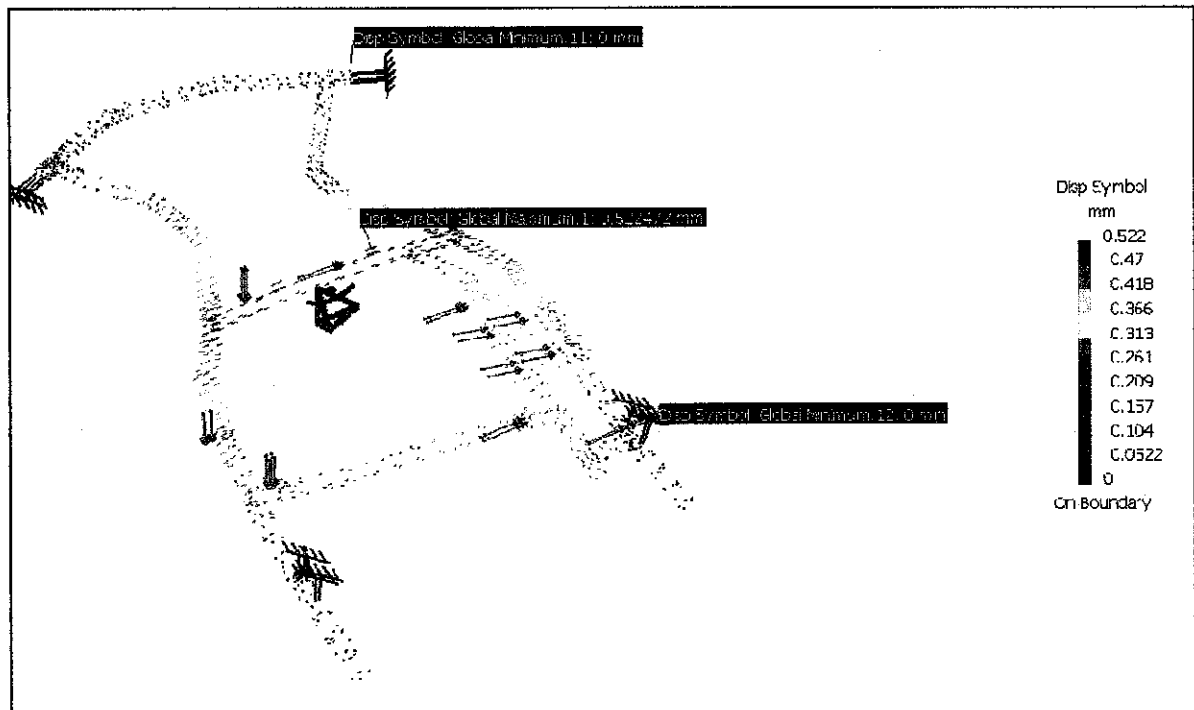
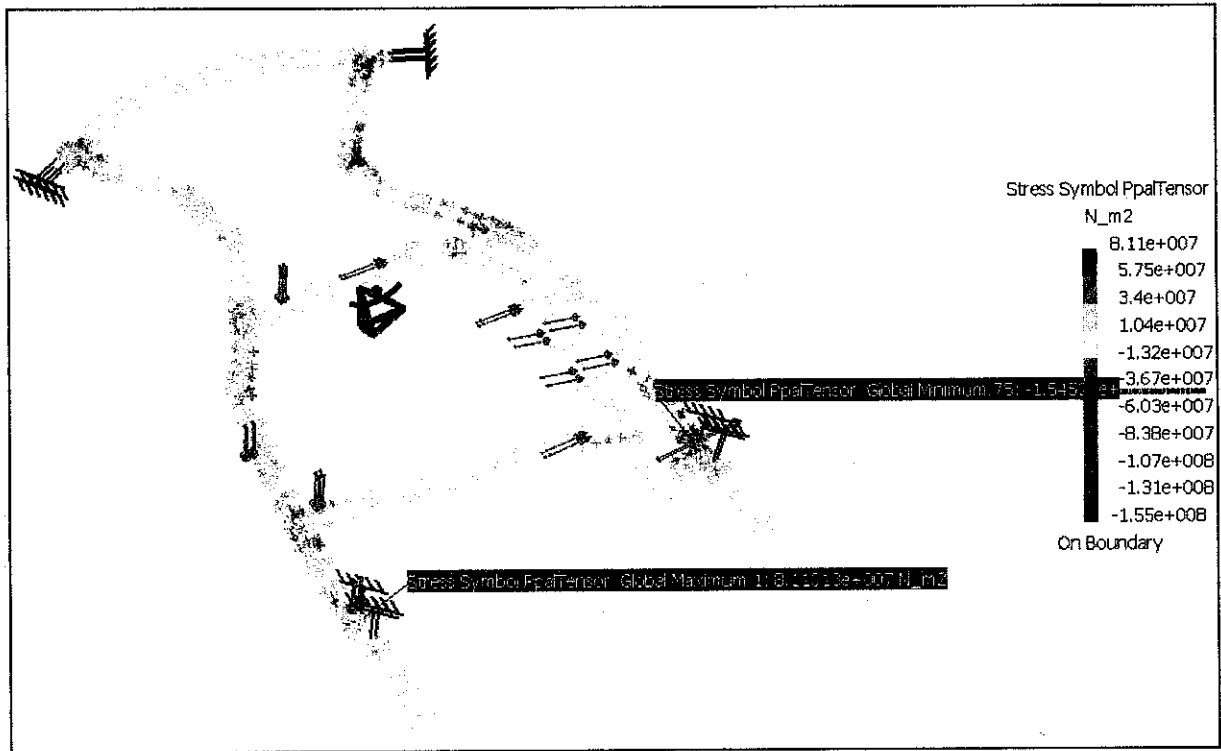


Figure 4.5.4 (b): Displacement Analysis on Chassis for Cornering (CW) Load Case



**Figure 4.5.4 (c): Principle Stresses Analysis on Chassis for Cornering (CW) Load Case**

**Table 4.5.4: Results for Cornering (CW) Load Case Analysis**

State Analysis	Measure	Location
Maximum Stress, $\text{Nm}^{-2}$	$2.21 \times 10^8$	Region of right rear axle joint with side frame
Maximum Displacement, mm	0.5520	Middle of centre frame
Principle Stresses, $\sigma$	Max $8.11 \times 10^7$ Min $-1.55 \times 10^8$	- Joint at right axle with side frame - Right side of rear axle joint with side frame

**4.5.5 CORNERING LOAD CASE (COUNTER-CLOCK WISE,  $a_c = 30ms^{-2}$ )**

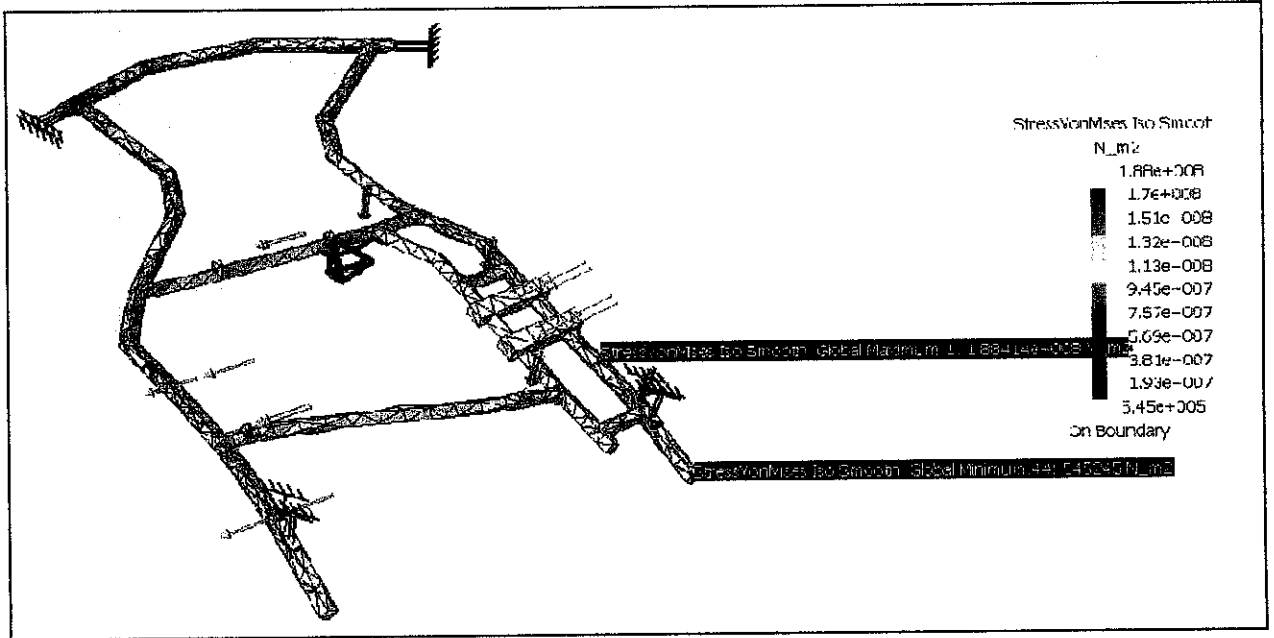


**Figure 4.5.5 (a): Stress von Mises Analysis on Chassis for Cornering (CCW) Load Case**

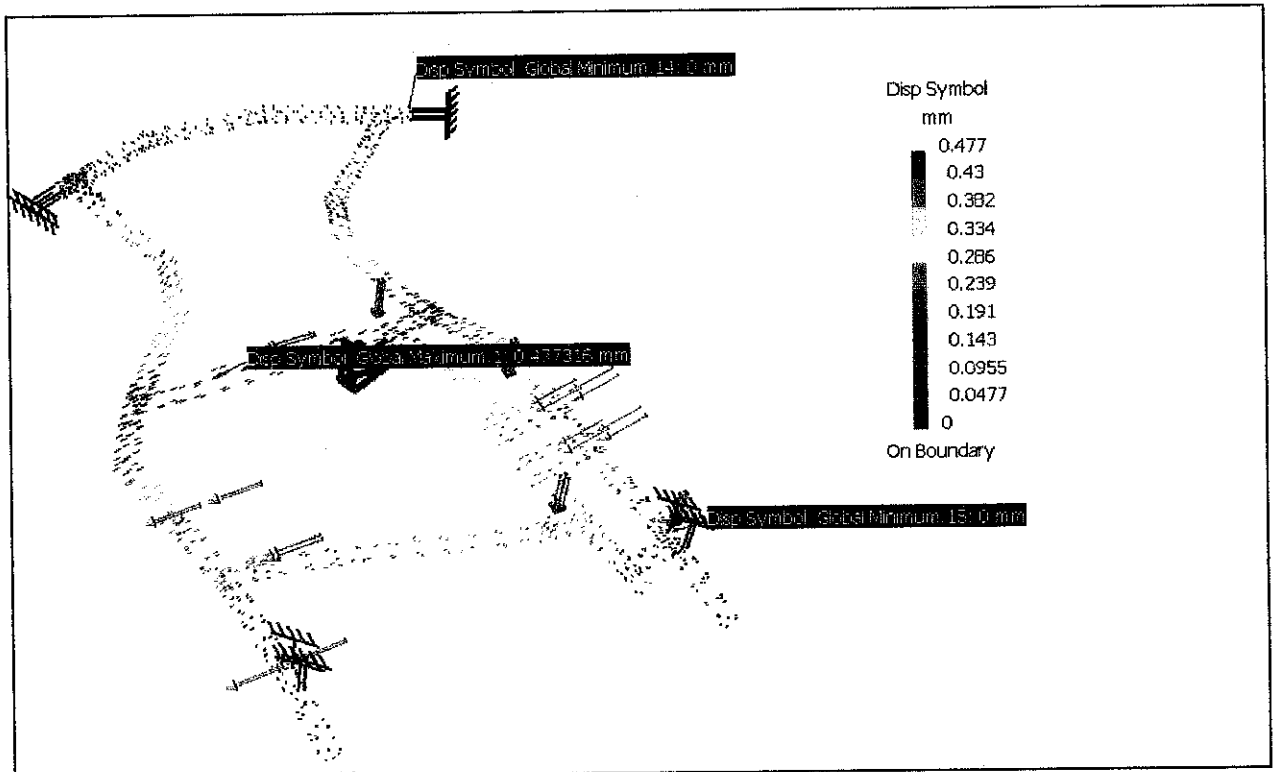


**Figure 4.5.5 (a): Displacement Analysis on Chassis for Cornering (CCW) Load Case**

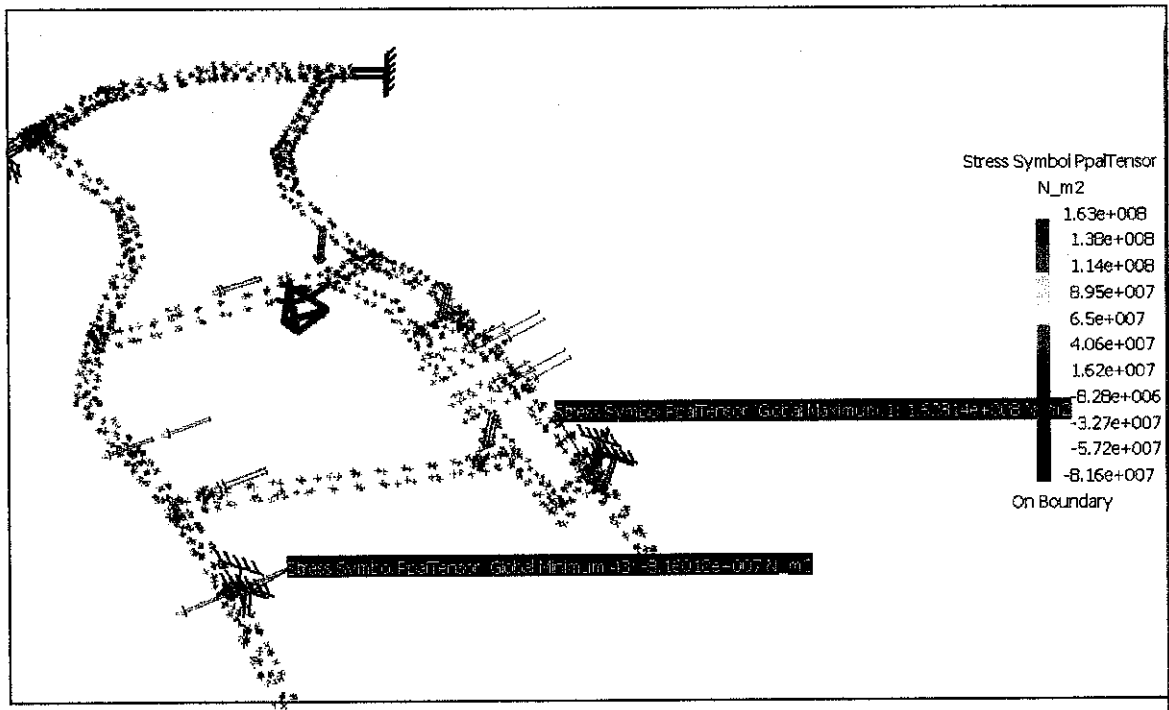


**Figure 4.5.5 (c): Principle Stresses Analysis on Chassis for Cornering (CCW) Load Case**

**Table 4.5.5: Results for Cornering (CCW) Load Case Analysis**

State Analysis	Measure	Location
Maximum Stress, $\text{Nm}^{-2}$	$1.88 \times 10^8$	Region of right rear axle joint with side frame
Maximum Displacement, mm	0.4770	Left middle of centre frame
Principle Stresses, $\sigma$	Max $1.63 \times 10^8$ Min $-8.16 \times 10^7$	- Joint at right axle with side frame - Joint of left rear axle with side frame

#### 4.5.6 POTHOLES LOAD CASE

The potholes effect is significant when one of the tires is in a free fall condition while the other is on flat surface. In this analysis, the previous frame proved inadequate to cater the forces built up because of these conditions. Then some modifications are made which is the addition of two torsion bars at front part of the chassis. These add on bars has significantly reduce the stress build up during pothole condition and also applies to bumps condition. On the reverse effect, the add on of two front torsion bars has cause the rear experience the greatest amount of stress build up. Although the maximum stress no more occurred at the front axle, the rear axle can absorb these stress and still within the yield strength of the material used. These additional torsion bars are actually just a bolt on bars for current market chassis. It is used in severe track condition with lots of bumps and potholes. For the purpose of this project and in controlling the cost of the project, these bars are welded together with the chassis.

The results of these analyses are according to the moment force built up at the bumped or potholed tire which is estimated around 3g of forces. The analyses were done based on constant velocity condition.

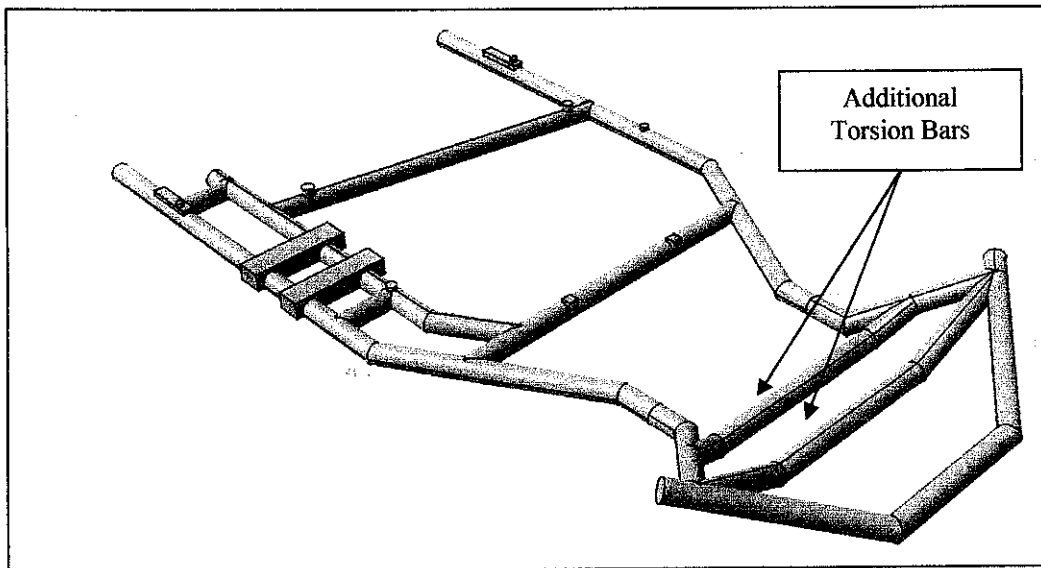


**Figure 4.5.6:** Go Kart Chassis with Two Front Torsion Bars

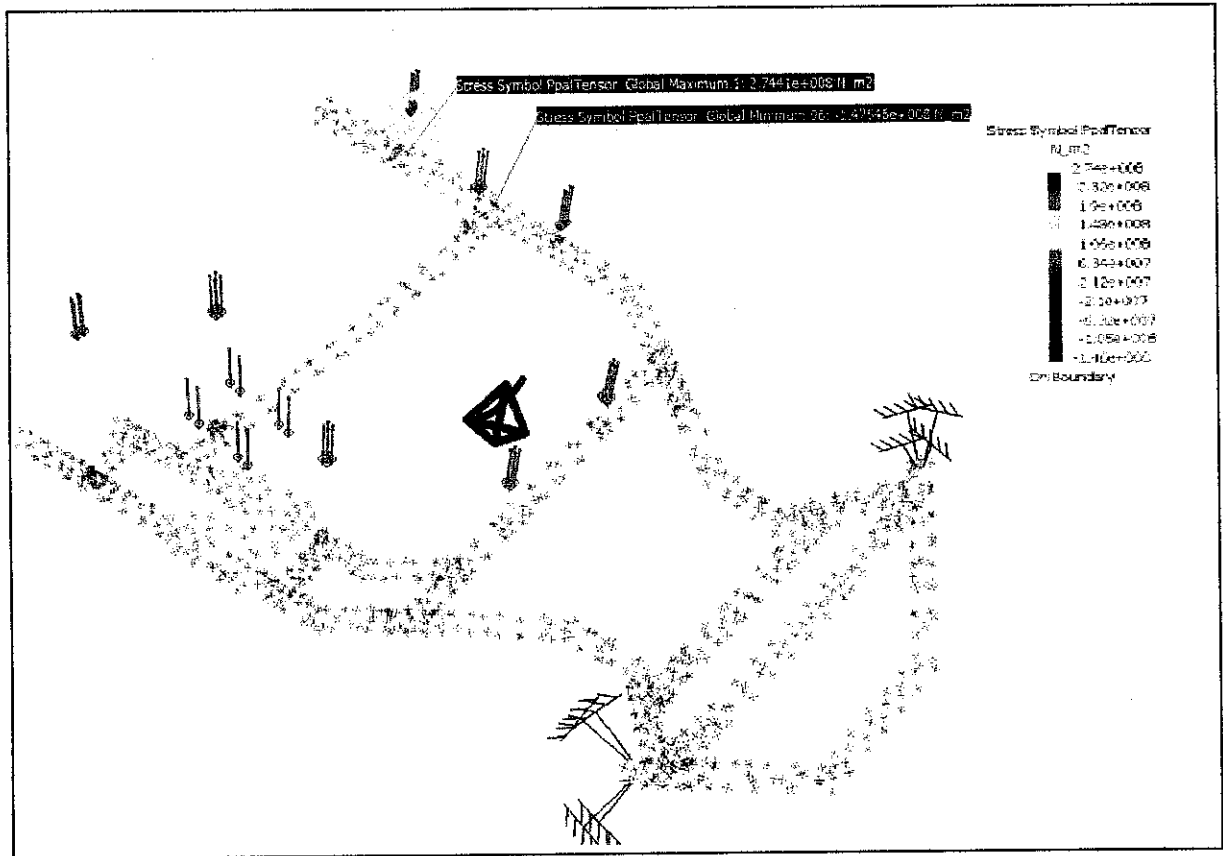


Figure 4.5.6 (c): Principle Stresses Analysis on Chassis for Potholes Load Case

Table 4.5.6: Results for Potholes Load Case Analysis

State Analysis	Measure	Location
Maximum Stress, $\text{Nm}^{-2}$	$2.68 \times 10^8$	Region of left rear axle joint with side frame
Maximum Displacement, mm	10.7043	Bottom right side frame
Principle Stresses, $\sigma$	Max $2.74 \times 10^8$ Min $-1.47 \times 10^8$	- Left rear axle joint to side frame - Joint of left side frame with cross tube

### 4.5.7 BUMPS LOAD CASE

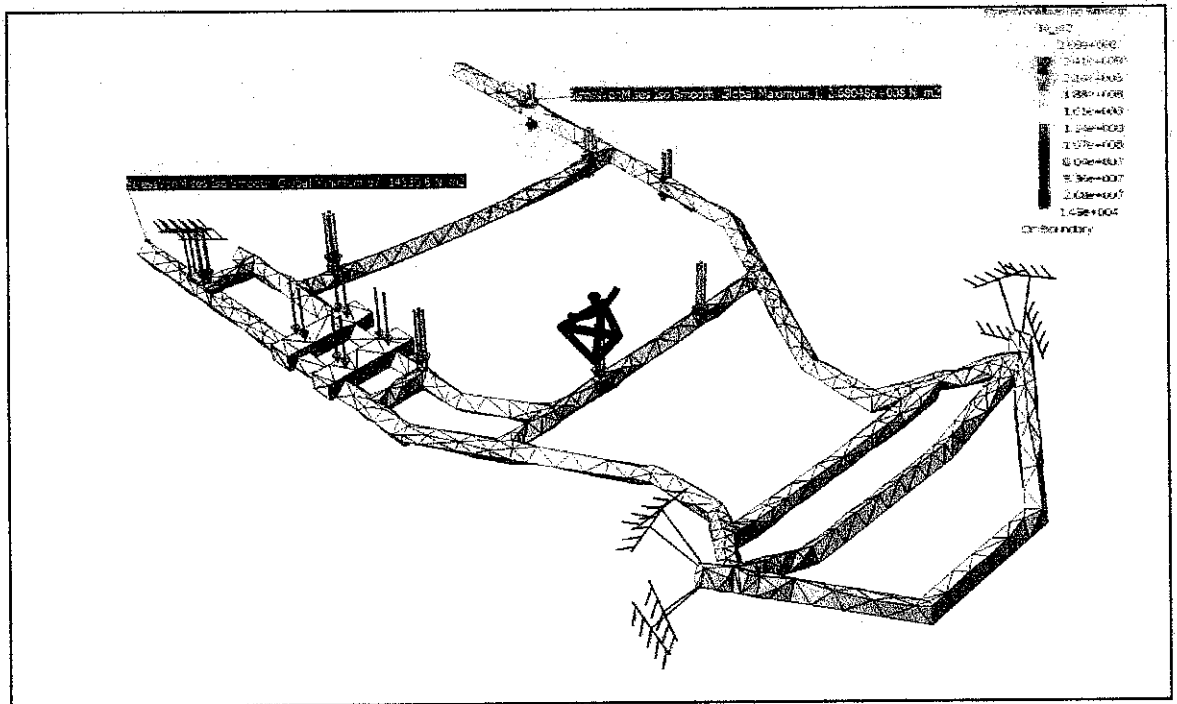


Figure 4.5.7 (a): Stress von Mises Analysis on Chassis for Bumps Load Case

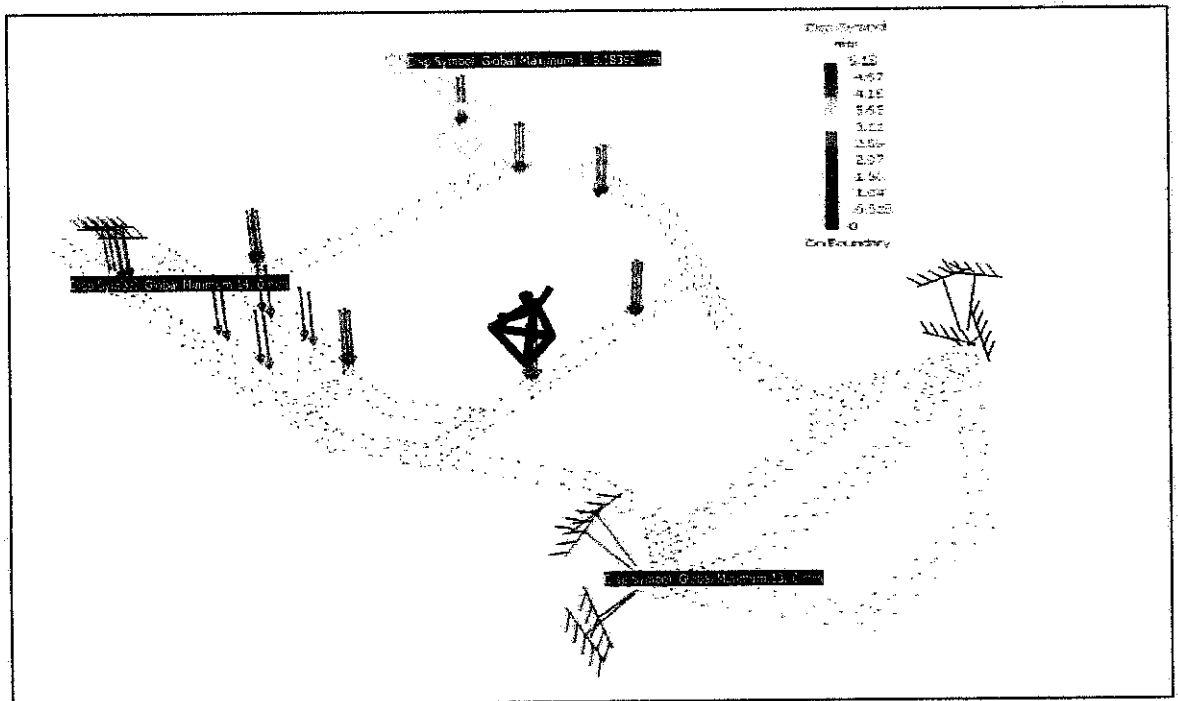


Figure 4.5.7 (b): Displacement Analysis on Chassis for Bumps Load Case

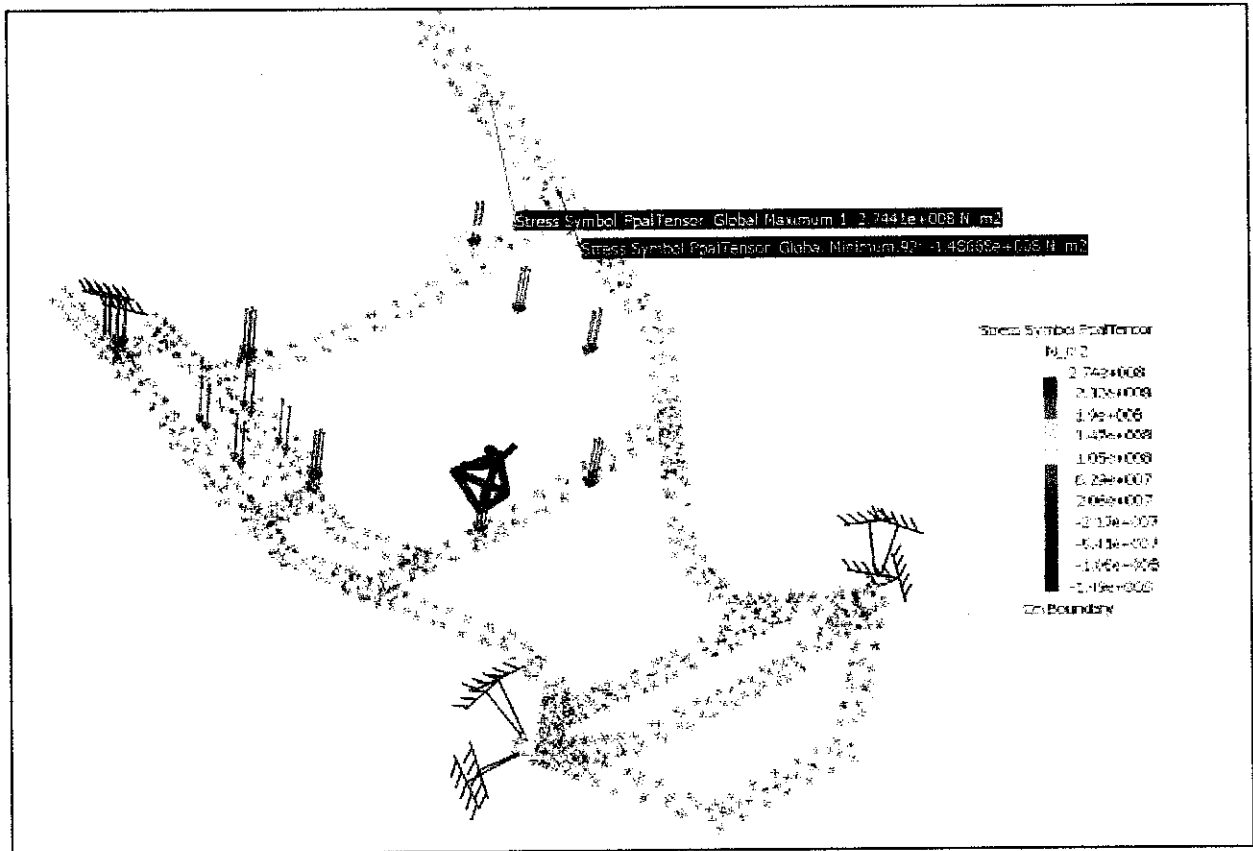


Figure 4.5.7 (c): Principle Stresses Analysis on Chassis for Bumps Load Case

Table 4.5.7: Results for Bumps Load Case Analysis

State Analysis	Measure	Location
Maximum Stress, $\text{Nm}^{-2}$	$2.68 \times 10^8$	Region of left rear axle joint with side frame
Maximum Displacement, mm	5.1839	Bottom left side frame
Principle Stresses, $\sigma$	Max $2.74 \times 10^8$ Min $-1.49 \times 10^8$	- Left rear axle joint to side frame - Joint of left side frame with cross tube

#### 4.6 Impact of Addition of Two Front Torsional Bars

Analysis that has been done by using the additional two front torsion bars also reflects the significant of adding such bars on go kart chassis. It affects the strength of the chassis whereby enable the chassis to resist greater stresses built up especially during bumps and potholes condition. For example, without the torsion bars, the chassis will experience a stress of  $5.70 \times 10^8 \text{ Nm}^{-2}$  at the front axle, which is higher than the yield strength of the material,  $3.80 \times 10^8 \text{ Nm}^{-2}$ . This great stress will fail the chassis under the bumps load condition. With the torsion bars, the chassis only experience stress of  $1.66 \times 10^8 \text{ Nm}^{-2}$ , which is well under the yield strength value. It is crucial to ensure the chassis design is able to withstand higher stresses during bumps and potholes. Without the bars, the chassis was found fails to avoid yielding to the material. The stresses built up in the chassis before the torsion bars were added in the potholes load case were found greater than the yield strength of the material used. Thus, to sustain such great stresses, the chassis was built complete with the two torsion bars to cater such condition.

Table 4.6 below summarizes the findings concerning the two front bars. The two front bars generally strengthen the front part of the chassis against potholes and bumps load cases in case of one of two front tire hit bumps or potholes.

**Table 4.6:** The increase of Chassis Strength by Adding Two Front Torsion Bars

Load Case	Yield Strength ( $\text{Nm}^{-2}$ )	Stress Without Two Torsion Bars ( $\text{Nm}^{-2}$ )	Stress With Two Torsion Bars ( $\text{Nm}^{-2}$ )	Percentage of Increase Strength (%)
<b>Bumps</b>	$3.80 \times 10^8$	$5.70 \times 10^8$	$1.66 \times 10^8$	344
<b>Potholes</b>	$3.80 \times 10^8$	$8.41 \times 10^8$	$1.96 \times 10^8$	430

#### 4.7 Final Design of Go Kart Chassis

The results from analysis are based on the point of load placed at certain mounting of essential parts or loads. These points of loads are driver's seat mounting, engine's mounting and also the petrol tanks. The final design of the chassis adding on the mountings for each load above is shown below.

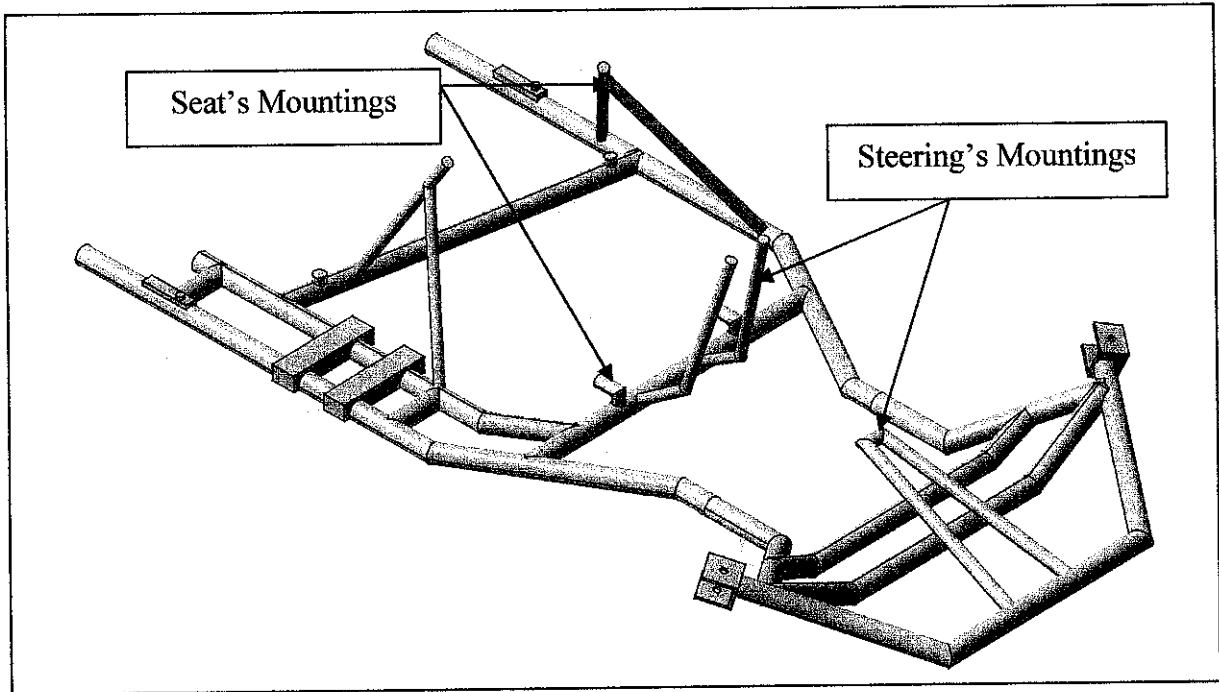


Figure 4.7 (a): Orthographic View of the Go Kart Chassis Final Design Complete with Mountings

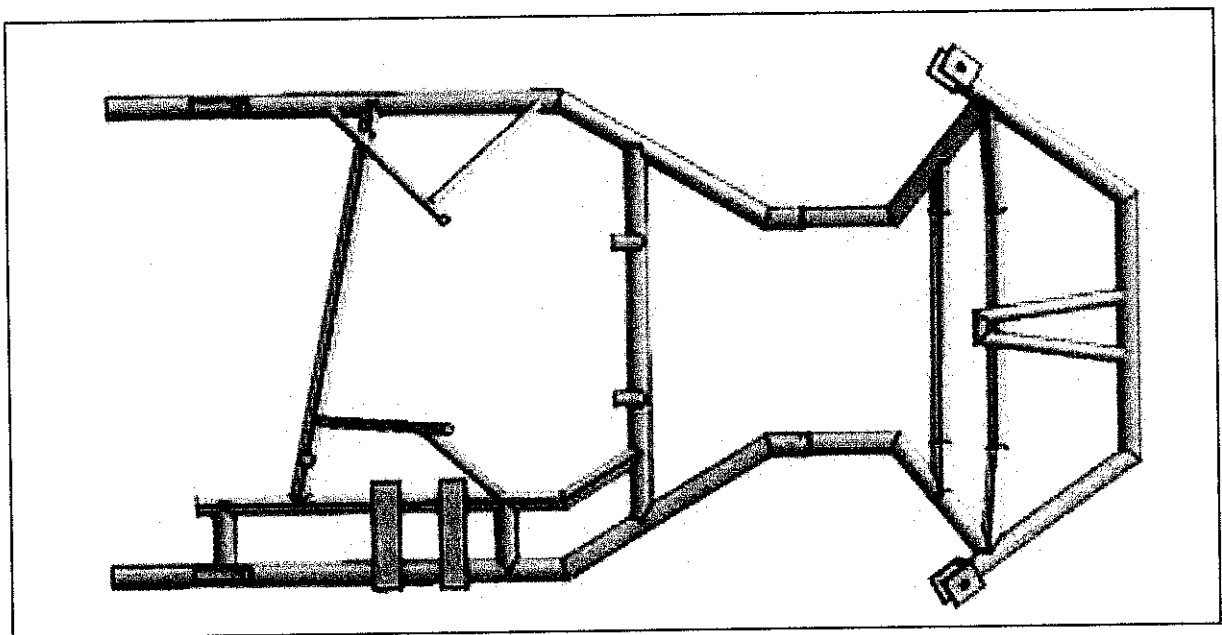


Figure 4.7 (b): Upper View of the Go Kart Chassis Final Design Complete with Mountings

## 4.8 Fabrication Phase

The chassis will be fabricated by using outsource manpower. This is due to lack of knowledge of the writer on welding up to the required standard. After discussing the issue with supervisor, it is agreed that the fabrication process will be done in workshops of experience welder with involvement of the writer. The limit cost for the chassis is RM1000 and this has set the actual cost of overall design and fabrication process of the chassis.

Once the final design with mountings completed, the design was then brought to manufacturer for fabrication. Upon selecting the manufacturer to fabricate the design, some crucial factors have to be determined. First of all is the cost of fabricating the go kart chassis according to the design. Second is the location of the workshop going to do the job. It is definitely preferable to have fabricator as closest to you as you can consult and observed the fabrication process on regular basis. These two factors are the most important factor, which decides which manufacturer will be selected to fabricate the chassis.

The other factors are the willingness to fabricate according to strict tolerance of  $\pm 5$  mm and also the experience of the welder. Time to complete the design also considered. After rigorous effort of founding the right welder and workshop, out of 5 possible workshop candidates evaluated, the workshop located at Taman Maju has been selected. The list of companies being surveyed and the selected workshop for the chassis fabrication is stated in the Appendix 4-8 (a).

After negotiations and deal has been reached upon the cost and time of completion, the fabrication process of the chassis commence under my supervision. After about 8 week, the chassis finally completed. The complete chassis fabricated is shown in Figure 4.8. The total cost for the fabrication process is RM 1000. Refer Appendix 4-8 (b) for cost details.

The size of welding throat,  $t$  was determined before the fabrication started. The calculation for the size of throat is shown in Appendix 4-8 (c). The throat size obtained, 4.5 mm is set to larger value during fabrication process ( $> 4.5$  mm). This measure is taken to ensure the weldments are strong to hold the joints together. This is also a safety precaution during welding process as

told by the workshop based on their experience. The welding positions involved were horizontal rolled (1G), horizontal weld (5G) and vertical (2G).

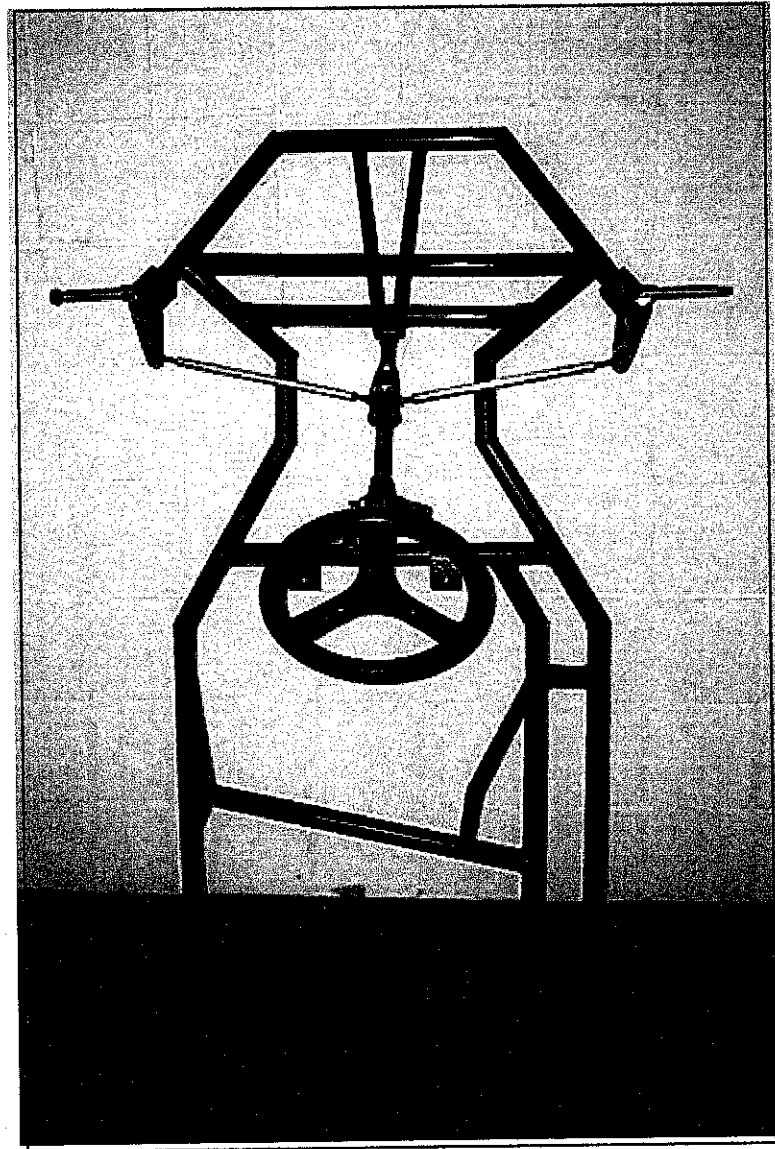


**Figure 4.8 (a):** Go Kart Chassis Fabricated Complete With Mountings, and Steering

### 4.9 Go Kart Chassis Homologation

Below is the homologation for the go kart chassis (Refer Figure 4.9 and Table 4.9).

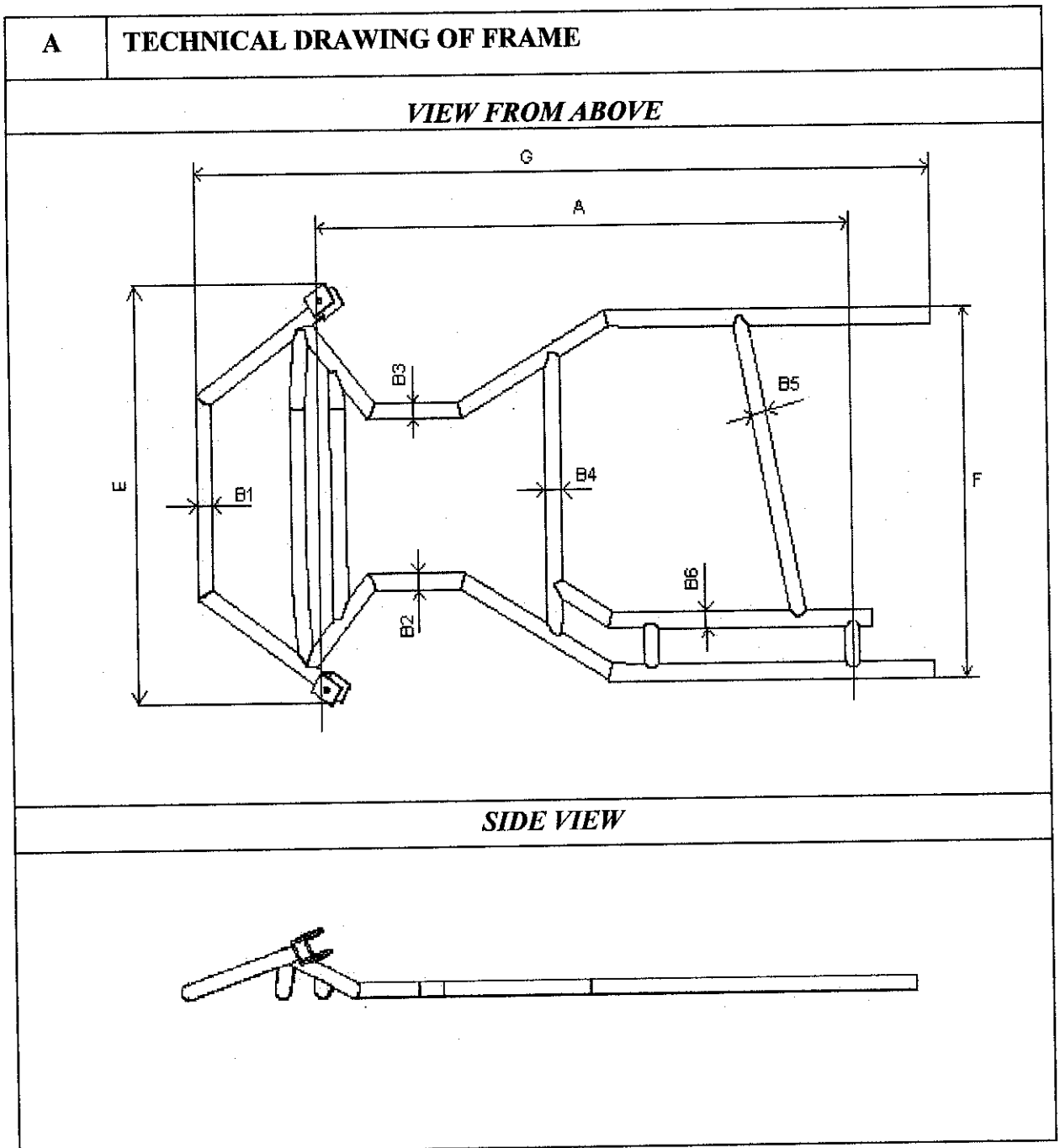


**Figure 4.9:** Go Kart Chassis Homologation for Upper View and Side View

**Table 4.9: Go-Kart Chassis Homologation (Dimensions)**

B	<i>DIMENSIONS</i>	
<i>Frame</i>	<i>Data</i>	<i>Tolerance</i>
A= Wheel base fixed measurement	1040 mm	±5 mm
B= Main tube of the structure main diameter 32mm, length over 1500mm, except lower tubes with a diameter 32mm and all the support for the accessories	1) 32 mm 2) 32 mm 3) 32 mm 4) 32 mm 5) 32 mm 6) 32 mm	±5 mm ±5 mm ±5 mm ±5 mm ±5 mm ±5 mm
C = Number of bend on the tube with diameter 32mm	15	
D = Number of tube with diameter over 32mm	-	
E = Outer front width	778 mm	±10 mm
F = Outer rear width	582 mm	±10 mm
G = Maximum outer overall length	1456 mm	±10 mm
Frame weight (including seat's and steering mounting)	15 kg	

#### 4.10 Testing on Chassis

The fabricated chassis has been undergone torsional rigidity test to compare the design rigidity in CATIA and the rigidity of the true completed chassis. The procedure of the testing and also the results are shown below.

### TORSIONAL RIGIDITY TEST PROCEDURE

**Title:**

Go Kart Chassis Torsional Rigidity

**Objective:**

To determine the go-kart chassis torsional rigidity (N/Degree) and compared to CATIA Simulation.

**Apparatus:**

A go-kart chassis, 2 clamp, weights (500g-5000g), vernier caliper, measuring tape

**Procedure:**

1. The go kart chassis was put into place. (Refer Figure 4.10 (a))
2. The rear axle of the chassis is clamped and make sure the clamp is strong enough to hold the chassis
3. Weight applied to the right front axle of the chassis with the increment of 500g.
4. The perpendicular distance, h of the axle travel downward and the distance x after the weight is applied is measured (Refer Figure 4.10 (b))
5. The value of h and x is recorded in Table 4.10.
6. Continue procedure 3 and 4 with increment of 500g of weight until 5 kg.
7. The data recorded is plotted in a Force, N versus Angle of Defection  $\theta$  (Graph 4.10).  
(The angle of deflection is obtained by using  $\tan^{-1} h/x = \theta$ )
8. Calculate the slope of the graph obtained.

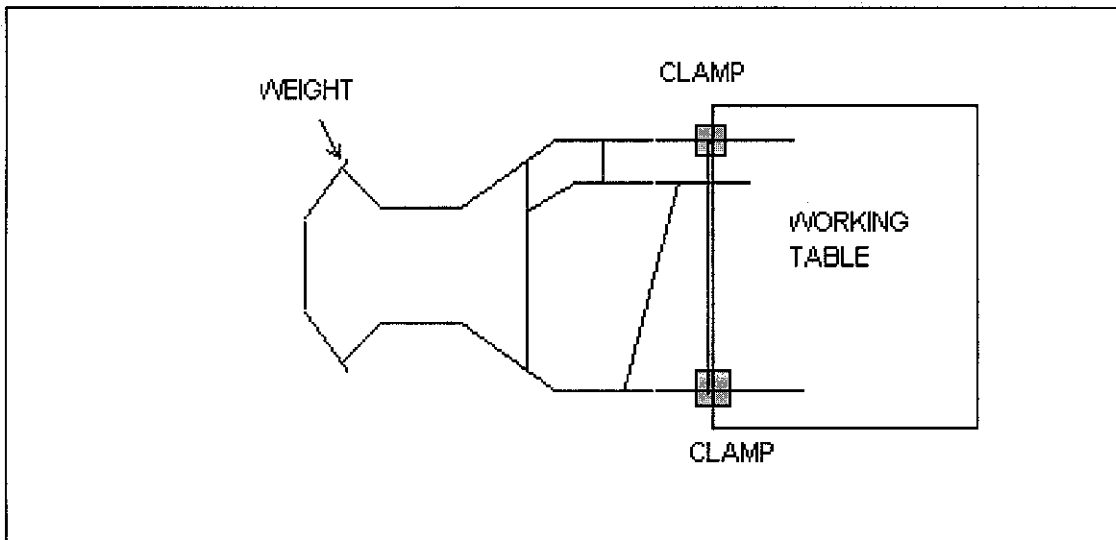


**Figure 4.10 (a):** The set up of the experiment

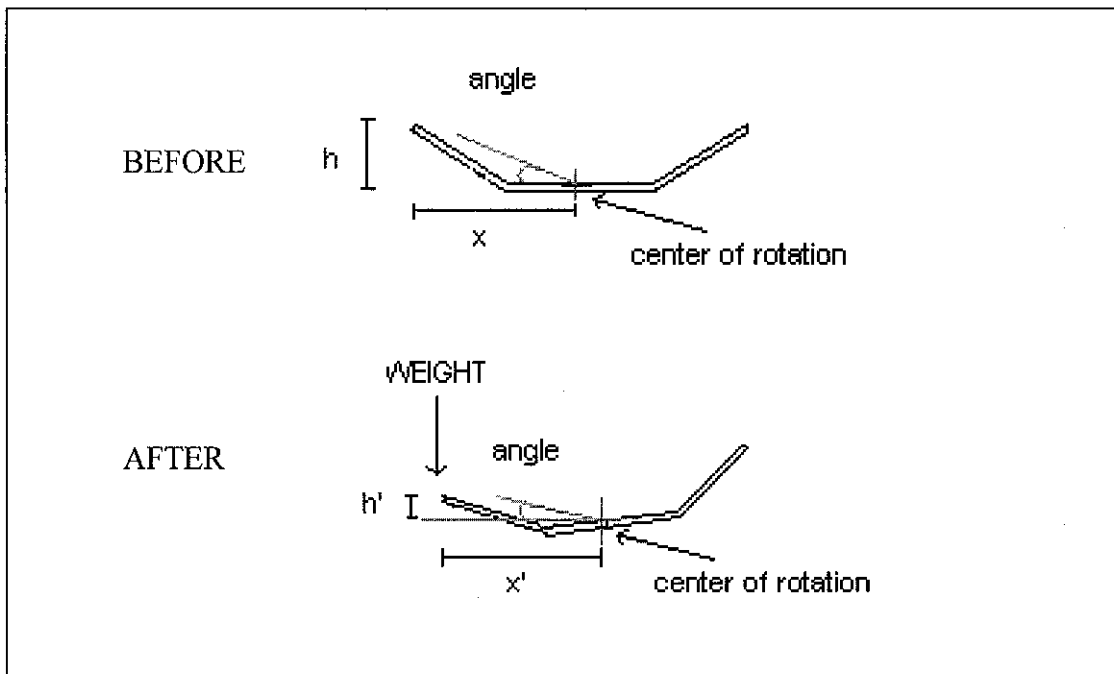


**Figure 4.10 (b):** The front view of the chassis before and after the weight is applied.

#### 4.10.1 Result of Torsional Rigidity Testing

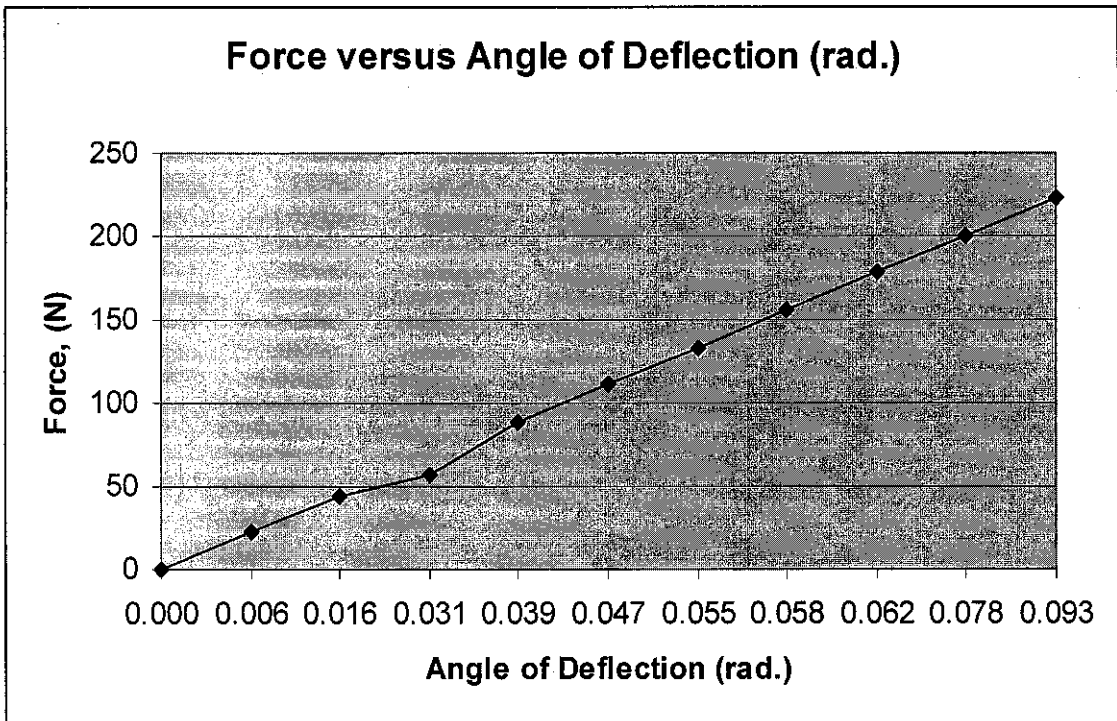
Mass, m (lb.)	Mass, m (kg)	Weight, N (Newton)	Displacement, h (mm)	Angle of Deflection, $\theta$ (rad.)
0	0	0	0	0
5	2.27	22.27	1.02.0	0.00625
10	4.54	44.54	5.0	0.015624
15	5.80	56.89	10.0	0.03124
20	9.07	88.98	12.5	0.039043
25	11.34	111.25	15.0	0.046841
30	13.61	133.51	17.5	0.054633
35	15.88	155.78	18.5	0.057748
40	18.14	177.95	20	0.062419
45	20.41	200.22	25	0.077967
50	22.68	222.49	30	0.093477

**Table 4.10:** Experiment Data for Torsional Rigidity Test

$$\begin{aligned} \text{Torsional Rigidity} &= \frac{222.49 \text{ N} (0.28 \text{ m})}{0.09377 \text{ rad}} \\ &= \mathbf{996.54 \text{ Nm/rad}} \end{aligned}$$

$$\text{Torsional rigidity test from FEA modeling} = \mathbf{1898.31 \text{ Nm/rad}} \text{ (Appendix 4-10-1)}$$

$$\begin{aligned} \text{Percentage of difference} &= \frac{(1898.31 - 996.54)}{1898.54} \times 100 \\ &= 47.49\% \end{aligned}$$



**Graph 4.10 (a):** Force, N vs. Angle of Deflection,  $\theta$  for Actual Chassis

#### 4.10.2 Conclusion from the Torsional Rigidity Test

From the torsional rigidity test, comparison between the theoretical value of the chassis rigidity tested in CATIA Simulation (FEA) and the actual rigidity from the real chassis can be seen. The difference between the values are 47.49%. In FEA test, the torque is exerted directly to the front axle. For actually testing, the forces are exerted on a beam and then calculation being made to evaluate the torsional rigidity. The beam should be rigid enough not to bend under applied forces. The difference exists because the material being used in the actual rigidity test as the beam has high ductility and tends to bend under small forces. The beam used is actually the beam used for weightlifting. Obviously, these types of beam tend to bend when the weight is lifted. This is what happens during the testing. This means that the beam would deflect more than the theoretical value obtained by FEA. Thus, giving it smaller torsional rigidity value. The other factor contributing to this difference is the welding itself. Welds are not uniformly made. This means that certain joint has bigger throat than other joint. This gives another strength distortion rather than a uniform strength of weld in FEA.

The test has successfully done and achieves its objectives. The actual torsional rigidity of the chassis obtained is 996.54 Nm/rad. It also identifies certain weakness on weld which is most probably cause by human error. From the torsional rigidity value obtained, one will know how much degree the chassis will bend when a certain force is applied.

## CHAPTER 5

### CONCLUSION AND RECOMMENDATION

Two type of common material used for constructing a go kart chassis; Aluminium Alloys 2024 and Mild Steel 1020 has been investigated and compared in term of weight, strength, manufacturability, ease of manufacturability and cost. Between these two metallic materials, Mild Steel 1020 has been chosen to be the most preferred alternatives for this project. Although the weight of aluminium is found 60% lighter than steel alloys, the cost and complicated fabrication process restricted the project to choose mild steel frame.

Constraint of cost and time for the project require other alternatives for frame tubular type. Go kart commonly use circular tube frame. But as for the ease of manufacturing and cost efficiency, rectangular tube frame has been considered. As the investigation on these two types of frame was done, still the circular tube frame was chosen.

The objective of designing and constructing a cheaper go kart chassis compared to the imports chassis has been achieve. The total cost for the go-kart chassis was RM 1000. This value is only for a single go kart prototype. For a larger number of quantities, this is best view in Appendix 5. From the graph, the value of RM 1000 for each go-kart represents the cost and profit. From the graph, as the quantity rises, the cost of the go-kart decreases. It can be as low as RM 800 if the quantity reaches the targeted 1000 units.

CATIA analysis familiarization has achieved its objective. Modification on the design has been done successfully to eliminate any weaknesses on the chassis by using the simulation. The significant strength increment of two front torsional bars proves these findings. Developments of engineering software definitely contribute to refinement of the chassis design.

Several recommendations subjected to improve the chassis design were considered. First, the vibration analysis of the chassis. The analyses are important to identify frequency and vibration rate of the chassis under determined condition to minimized any fatigue stress that may disrupt

the chassis structure. Second, the weld joint made from Tungsten Inert Gas (TIG) is found preferable for tube structure but because of the cost constraint, MIG was used instead. The third recommendation is research on the best material for constructing the chassis. Material actually being used in making the current chassis in the market is still mysterious since it is a confidential data of the manufacturer. The construction of jigs also could enhance the accuracy of the chassis dimension and ease of fabrication, thus minimizing fabrication time for numerous number of chassis production. These recommendations should be considered for further enhancement of the go-kart chassis design and fabrication.

Go kart industry in Malaysia slow growth is closely related to the consumer buying power, which is quite low. This is because the spare parts and mainly chassis imported are expensive and the buying process could be a troublesome for new people in the industry. Development of go kart chassis locally could rapidly improve the go-kart industry in Malaysia. It allows enthusiast a new option, which is less expensive, yet improved design; light, strong and comply with the FIA regulation. Hopefully, this project will be a platform for further go-kart chassis development in our country.

## CHAPTER 6

### REFERENCES

1. book refer to Ferdinand P. Beer and E. Russel Johnson Jr. (1992)
2. book refer to William D. Calister Jr. (2003)
3. book refer to Robert W. Messler Jr. (1999)
4. book refer to Hoobasar Rampaul (2003)
5. book refer to John Hicks (1999)
6. book refer to S. J. Maddox. (2002)
7. website refer to Morac (2003)

Ferdinand P. Beer, E. Russell Johnson, Jr. 1992, *Mechanics of Material*, New York McGraw-Hill

William D. Callister, Jr. 2003, *Materials Science and Engineering*, New York, Wiley International

Robert W. Messler Jr. 1999, *Principles of Welding Processes, Physics, Chemistry, and Metallurgy*, New York, Wiley-Interscience

Hoobasar R. 2003, *Pipe Welding Procedures*, New York, Industrial Press

Hicks, J. 1999, *Welded Joint Design*, Cambridge Abington Publishing

Maddox, S. J. 2002, *Fatigue Strength of Welded Structure*, Cambridge, Abington Publishing

Duncan, Donna. Dec 2003 <[http:// www.morac.com/index1.html](http://www.morac.com/index1.html) >.

Klein-Smith, Sarah. 6 Sept 1998 <http://members.aol.com/~skmorac2/>

**Table 1.3: Milestone for the First Semester of 2 Semester Final Year Project**

No.	Detail/ Week	1	2	3	4	5	6	7	8	9	10	11	12	13	14
1	Selection of Project Topic	█													
	-Propose Topic														
	-Topic assigned to students														
2	Preliminary Research Work	█													
	-Introduction														
	-Objective														
	-List of references/literature														
	-Project planning														
3	Submission of Preliminary Report		●												
4	Project Work			█											
	-Reference/Literature														
	-Chassis Design Measurement and Evaluation														
	-Visit to Go Kart Workshop														
	-Final Design for Go Kart Chassis														
5	Submission of Progress Report							●							
6	Project work continue							█							
	- Catia Analysis, FEA, Stress Analysis														
	-Material Selection														
7	Submission of Interim Report Final Draft												●		
8	Oral Presentation													●	
9	Submission of Interim Report														●

No.	Detail/ Week	1	2	3	4	5	6	7	8	9	10	11	12	13	14
1	Project Work Continue														
	-Fabrication Methods Define														
	-Fabrication Planning														
2	Submission of Progress Report 1														
3	Project Work Continue														
	-Fabrication Continue														
4	Submission of Progress Report 2														
5	Project work continue														
	- Fabrication Continue														
	- Chassis Assembly and Testing														
6	Submission of Dissertation Final Draft														
7	Oral Presentation														
8	Submission of Project Dissertation														

● Suggested milestone  
 ■ Process

APPENDIX 2-1 (a)

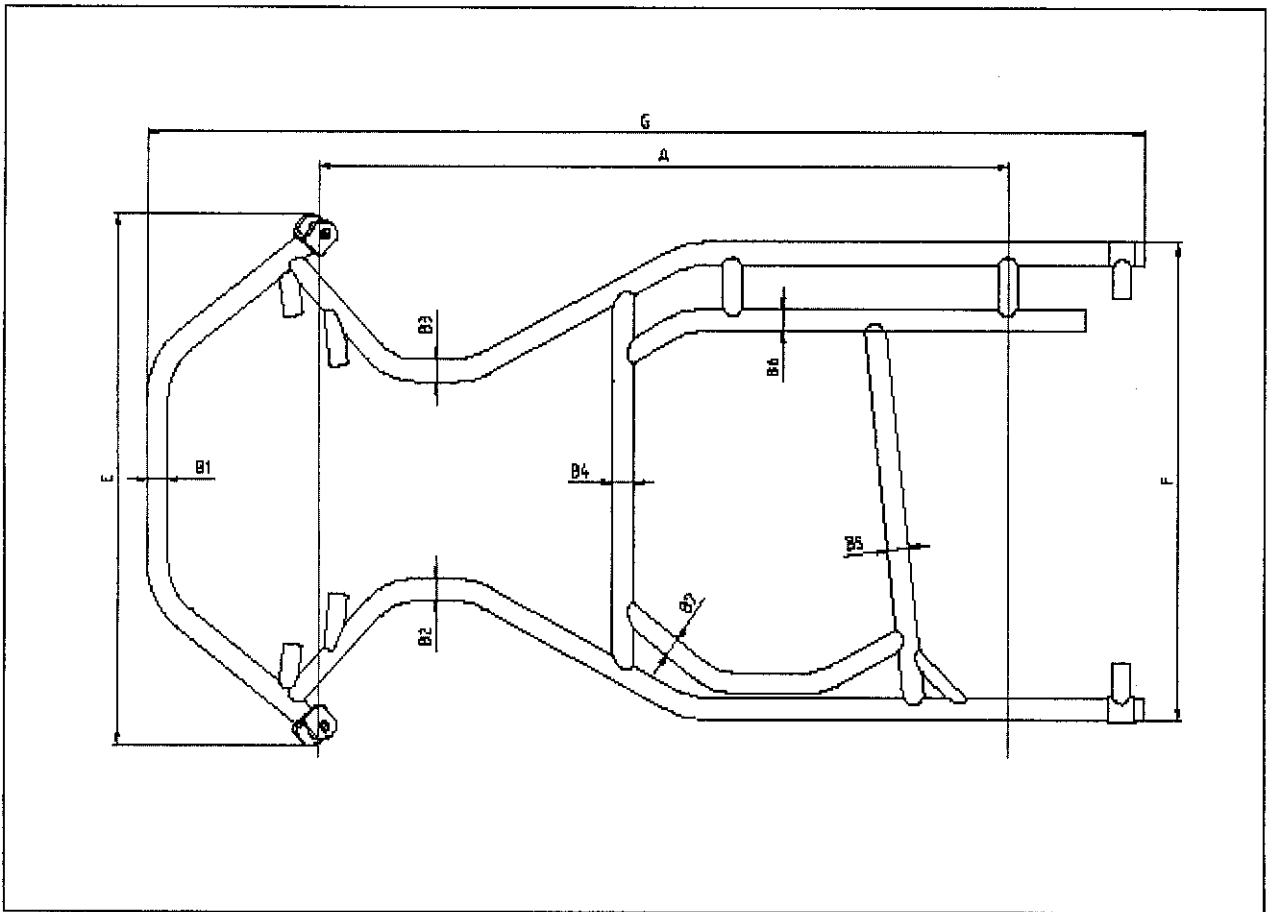


Figure 2.1 (a): Technical Drawing of Frame Subjected to FIA Homologation



APPENDIX 2-1 (c)

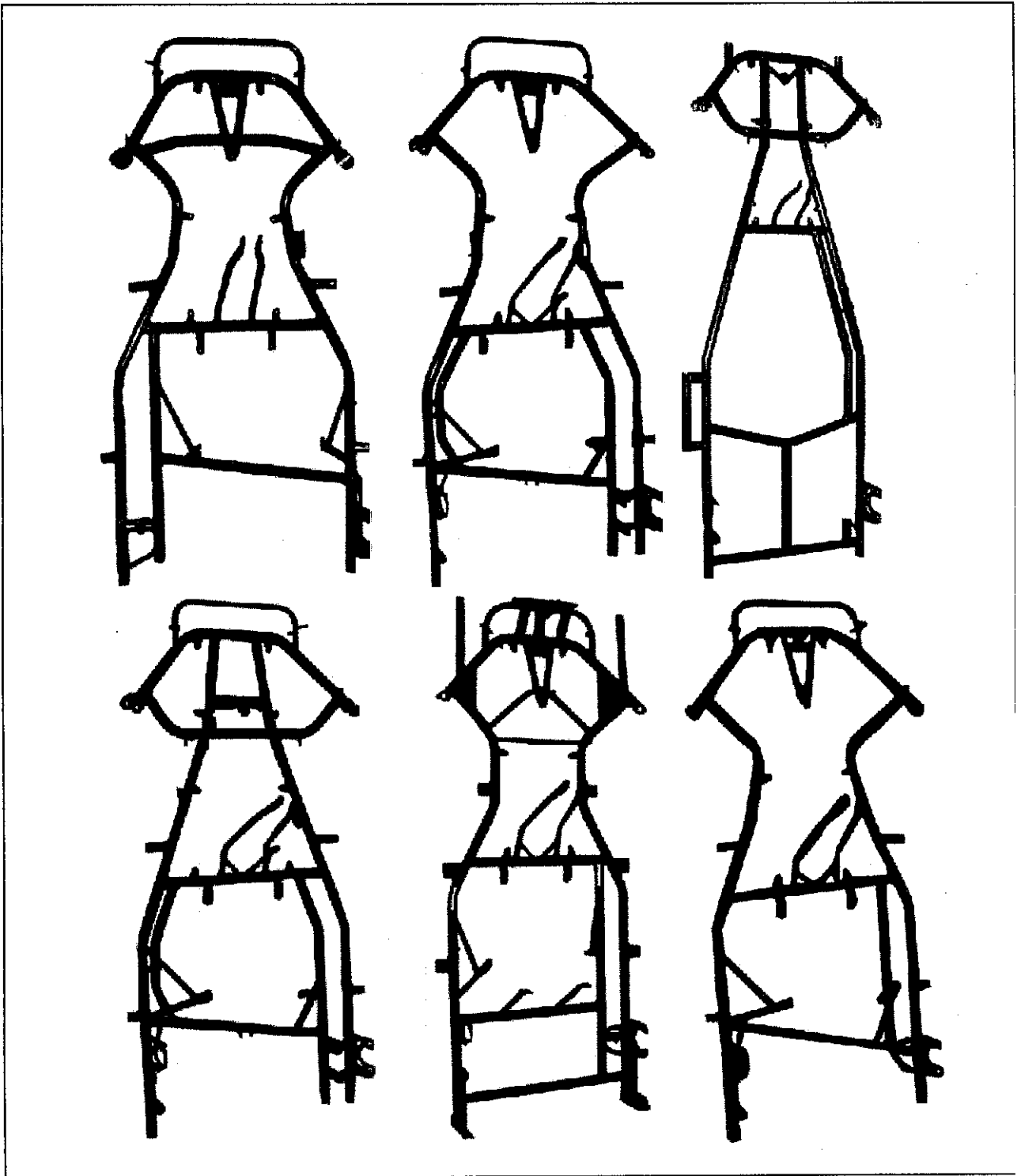


Figure 2.1 (c): Samples of Current Go Kart Chassis Design in the Market (Azzuries Series)

APPENDIX 3-2

**Table 3.2: The Specifications and Description of Welding Process**

Welding Specification	Description
Welding type	Gas Metal Arc Welding (GMAW/MIG)
Models	WIM Welding Product: MigWeld 210 EF
Shielding Gas	Carbon Dioxide, CO <sub>2</sub>
Voltage (Used), V	10 V – 45 V (20 V)
I <sub>max</sub> (Used), I	105 A (35 A)
Electrode wire diameter	0.8 mm
Electrode wire classification	AWS A5 (18ER70 S4)
Wire feed rate	2.5 m/min
Filler Yield Strength	415 MPa
Type of molten metal transfer	Bridging/Short-circuit transfer mode (Repelled)
Throat size, t	> 5 mm

APPENDIX 4-8 (a)

Table 4.8 (a): List of Companies Surveyed and Fabrication Specifications (Company in bold is selected)

Company	Location	Cost Demanded (RM)	Time of Completion (Weeks)	Tolerance (mm)	Recommendation (Yes/No)
Seng Lee Engineering Works Sdn. Bhd.	Papan Industrial Park	3000	8	10	No (Cost limit)
Precise Elegance Sdn. Bhd.	Menglembu Industrial Park	3500	8	10	No (Cost limit)
<b>Gang Enterprise</b>	<b>Taman Maju, Tronoh</b>	<b>1000</b>	<b>8</b>	<b>10</b>	<b>Yes</b>
Fook Engineering Works	Menglembu Industrial Park	3500	8	5	No (Cost limit)
Thiang Engineering Works	Menglembu Industrial Park	4000	8	10	No (Cost Limit)

APPENDIX 4-8 (b)

**Table 4.8 (b): Cost Detail for Go-Kart Chassis Fabrication**

Bill of Material	Description	Cost (RM)
Material (Mild Steel 1020)	6m x 2	40
Consumable Electrode	AWS A5 (18 ER70 S-4) - 1 roll	60
Labor Cost	2 person - chassis bare frame - chassis accessories (mountings)	500 400
<b>Total Cost</b>		<b>1000</b>

APPENDIX 4-8 (c)

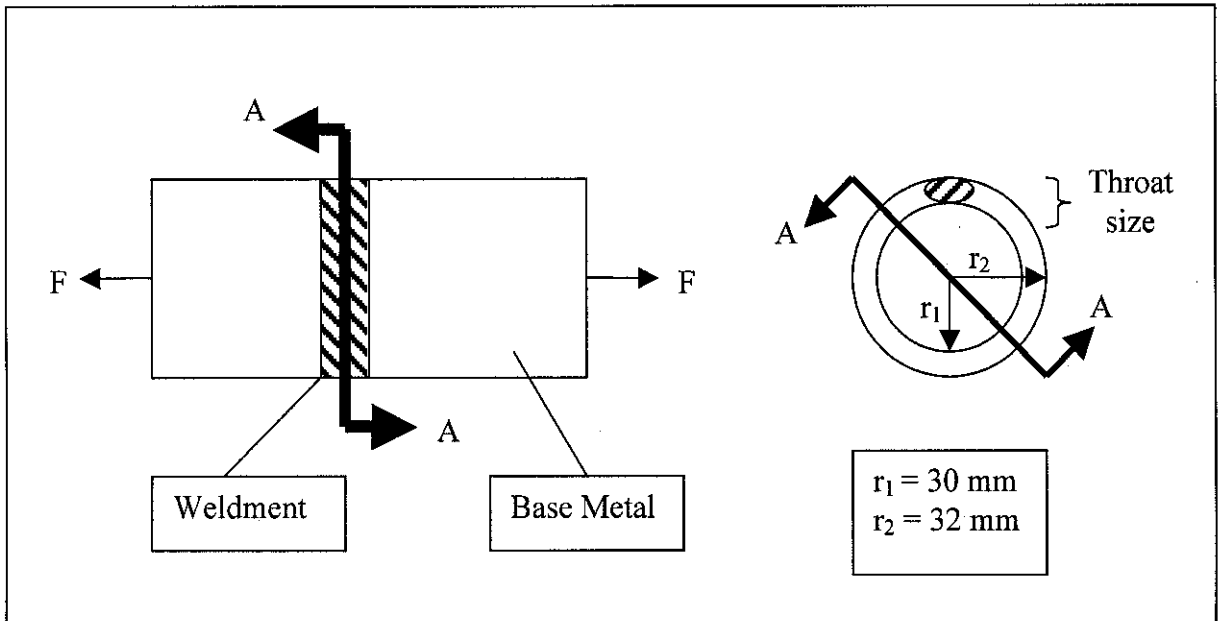


Figure 4.8 (b): Schematic Diagram for Calculating Throat Size,  $t$  for the Weldment

Formula:

$$\text{Throat size, } t = \frac{F}{S \times \sigma_{\text{weld}} \times L}$$

Where,

$F$  = Force at weldment, (N)

$\sigma_{\text{weld}}$  = Allowable stress for weld material, (MPa)

$L$  = Length of weldment, (m)

$S$  = Safety Factor

Value of F at the weld is set equals to material yield strength. This is because the weld yield strength (415 MPa) is greater than the base material yield strength (380 MPa). Safety factor, S is set to 3 referring to “ANSI/AWS D1.1-90 Section 1 through 7, Section 8 where applicable...”, “...and the Commentary on Structural Welding Code – Steel, (Part of ANSI/AWS D1.1)”.

$$\begin{aligned}
 F &= \frac{\sigma_{\text{base}}}{\text{Area}} \\
 &= \frac{380 \times 10^6 \text{ Nm}^{-2}}{\pi (0.32^2 - 0.30^2) \text{ m}} \\
 &= 1.48 \times 10^7 \text{ N}
 \end{aligned}$$

$$\begin{aligned}
 \text{Throat size, } t &= \frac{1.48 \times 10^7 \text{ N}}{1/3 \times 4.95 \times 10^8 \text{ Nmm}^{-2} (2 \pi \times 0.32 \text{ m})} \\
 &= 0.04461 \text{ m} \\
 &= 4.461 \text{ mm} \approx \mathbf{4.5 \text{ mm}}
 \end{aligned}$$

**APPENDIX 4-10-2**

Formula:

$\text{Torsional Rigidity, } \sigma = \frac{T}{57^\circ} \times \frac{L}{\theta}$
---

T = torque, Nm

L = spread length, m

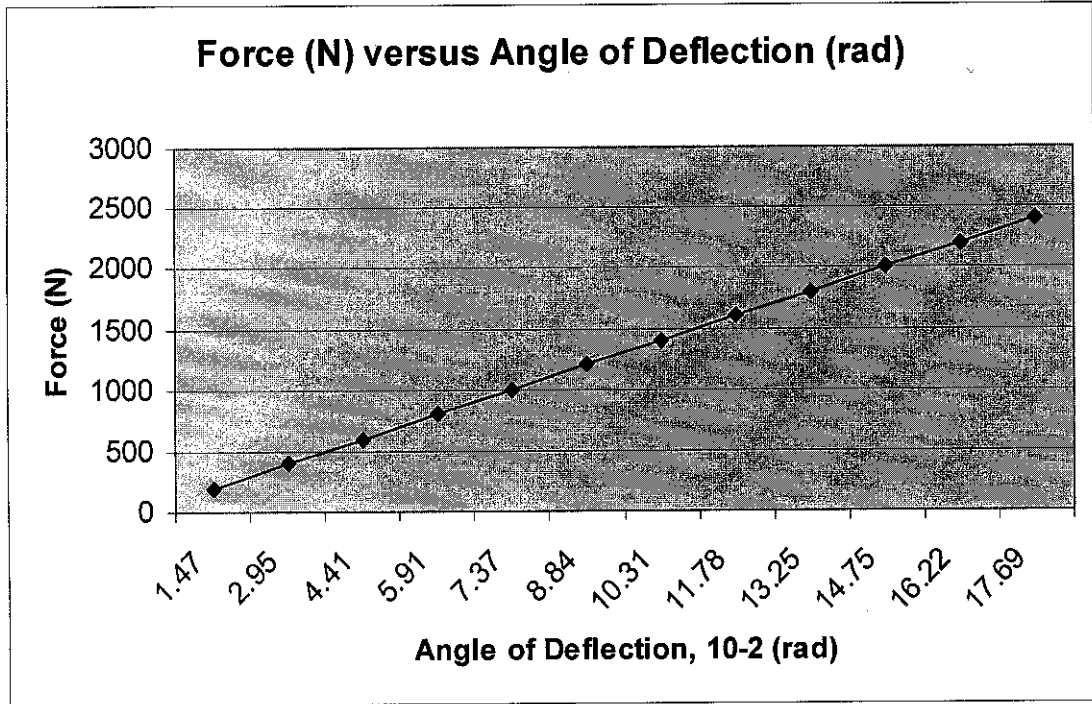
θ = deflection, m

**CATIA Simulation Results:**

**Table 4.10 (b): Forces, F (N) Applied and the Related Angle of Deflection, θ (rad)**

Force, F (N)	Displacement, h (m)	Angle of Deflection, θ (rad) (10 <sup>2</sup> )
200	0.472	1.47
400	0.943	2.95
600	1.41	4.41
800	1.89	5.91
1000	2.36	7.37
1200	2.83	8.84
1400	3.3	10.31
1600	3.77	11.78
1800	4.24	13.25
2000	4.72	14.75
2200	5.19	16.22
2400	5.66	17.69

APPENDIX 4-10-2



**Graph 4.10 (b):** Force, F (N) versus Angle of Deflection,  $\theta$  (rad) for CATIA Simulation

Take value at force exerted 2000 N,

$$\begin{aligned} \text{Torsional Rigidity} &= \frac{2000 \text{ N} (0.28 \text{ m})}{2 (0.1475 \text{ rad})} \\ &= \mathbf{1898 \text{ Nm/rad}} \end{aligned}$$

**Actual Chassis Torsional Rigidity (as per Table 4.10);**

Taking value at 50 lb.

$$\begin{aligned} \text{Torsional Rigidity} &= \frac{222.49 \text{ N} (0.42 \text{ m})}{0.09377 \text{ rad}} \\ &= \mathbf{996.54 \text{ Nm/rad}} \end{aligned}$$

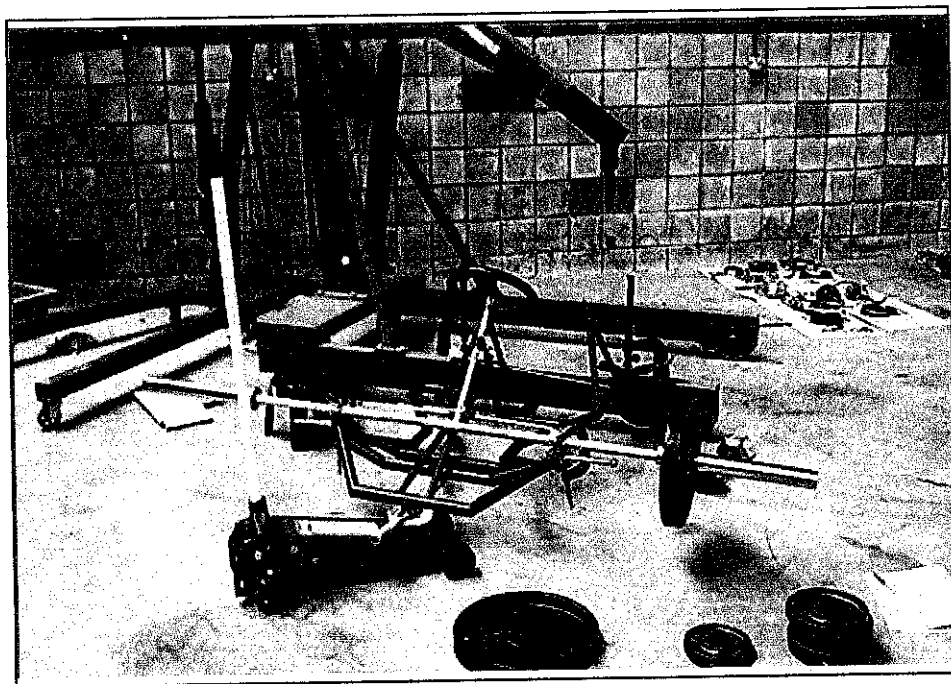


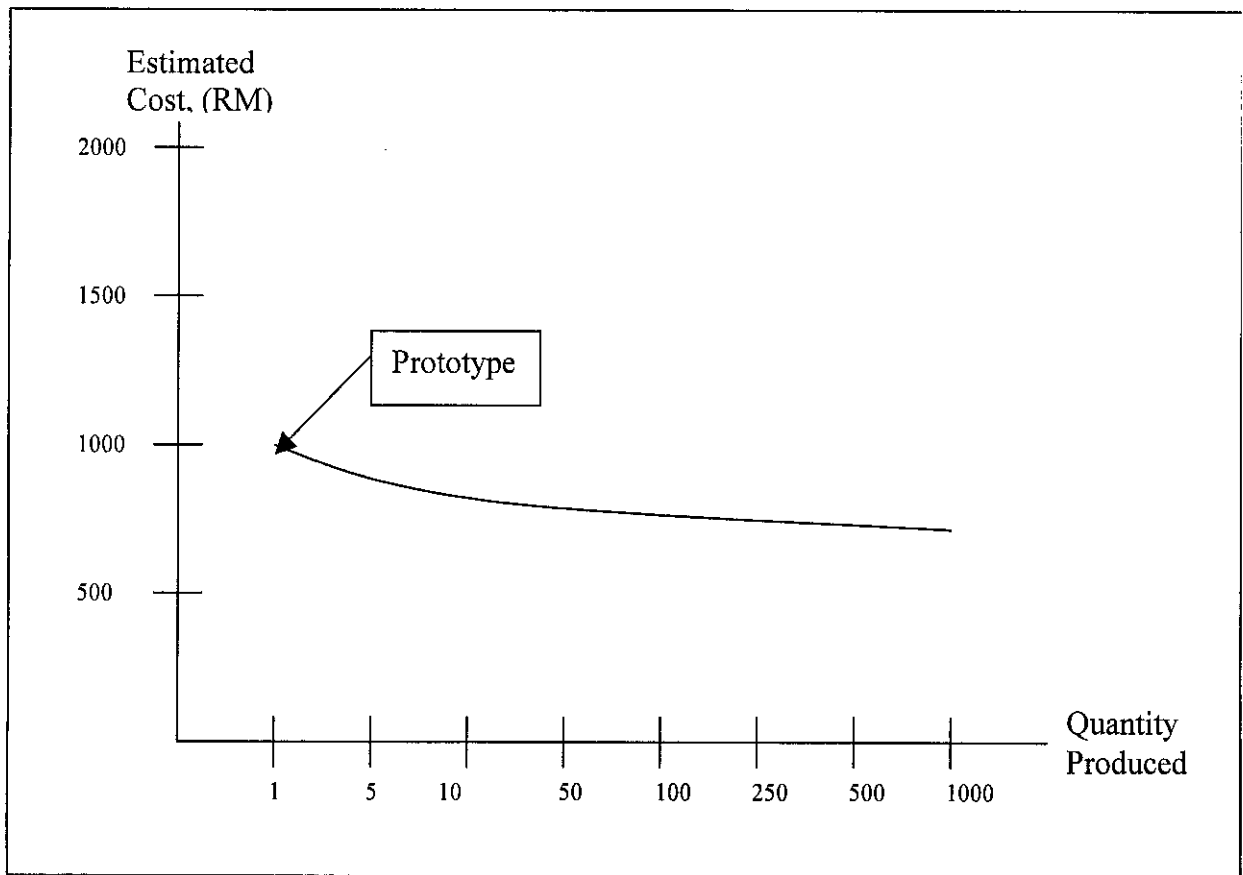
Figure 4.10 (c)



Figure 4.10 (d)

Figure 4.10 (c) and (d): The Chassis Set Up for Torsional Rigidity Test

## APPENDIX 5-0



**Graph 5.0:** Cost versus Quantity for Go Kart Chassis

### NOTE:

- 1) The prototype cost (RM 1000) is including the buying of new filler and 6m x 2 pieces of mild steel tubing.
- 2) This same filler stock could make up at least 10 go kart chassis.
- 3) The reduction in total cost relate to the labor cost of constant production.
- 4) This in turn gives the labor a constant salary for production, not depend on the production rate.
- 5) The decrease curve also reflects the cost of material used such as Mild Steel and also the filler used.
- 6) The cost does not include the maintenance on the GMAW machine.